Accepted Manuscript

Synthesis and bio-evaluation of indole-chalcone based benzopyrans as a promising antiligase and antiproliferative agent

Sampa Gupta, Pooja Maurya, Akanksha Upadhyay, Pragati Kushwaha, Shagun Krishna, Mohammad Imran Siddiqi, Koneni V. Sashidhara, Dibyendu Banerjee

PII: S0223-5234(17)30908-X

DOI: 10.1016/j.ejmech.2017.11.015

Reference: EJMECH 9890

To appear in: *European Journal of Medicinal Chemistry*

Received Date: 6 July 2017

Revised Date: 16 October 2017

Accepted Date: 4 November 2017

Please cite this article as: S. Gupta, P. Maurya, A. Upadhyay, P. Kushwaha, S. Krishna, M.I. Siddiqi, K.V. Sashidhara, D. Banerjee, Synthesis and bio-evaluation of indole-chalcone based benzopyrans as a promising antiligase and antiproliferative agent, *European Journal of Medicinal Chemistry* (2017), doi: 10.1016/j.ejmech.2017.11.015.

This is a PDF file of an unedited manuscript that has been accepted for publication. As a service to our customers we are providing this early version of the manuscript. The manuscript will undergo copyediting, typesetting, and review of the resulting proof before it is published in its final form. Please note that during the production process errors may be discovered which could affect the content, and all legal disclaimers that apply to the journal pertain.

ACCEPTED MANUSCRIPT

Graphical abstract

Synthesis and bio-evaluation of indole-chalcone based benzopyrans as a promising antiligase and antiproliferative agent

Sampa Gupta[1†], Pooja Maurya[2†], Akanksha Upadhyay[1], Pragati Kushwaha[1], Shagun Krishna[2], Mohammad Imran Siddiqi[2#], Koneni V. Sashidhara*[1#], Dibyendu Banerjee*[2#]

[1]Medicinal and Process Chemistry Division, [2]Molecular and structural biology division,

Academy of Scientific and Innovative Research (AcSIR), India

† Both authors contributed equally to this work.

CSIR-Central Drug Research Institute, (CSIR-CDRI), BS-10/1, Sector 10, Jankipuram Extension, Sitapur Road, Lucknow, 226031, India.

*Correspondence and requests for materials should be addressed to D.B (d.banerjee@cdri.res.in, dibyenducdri@gmail.com) and K.V.S (e-mail: sashidhar123@gmail.com, kv_sashidhara@cdri.res.in)

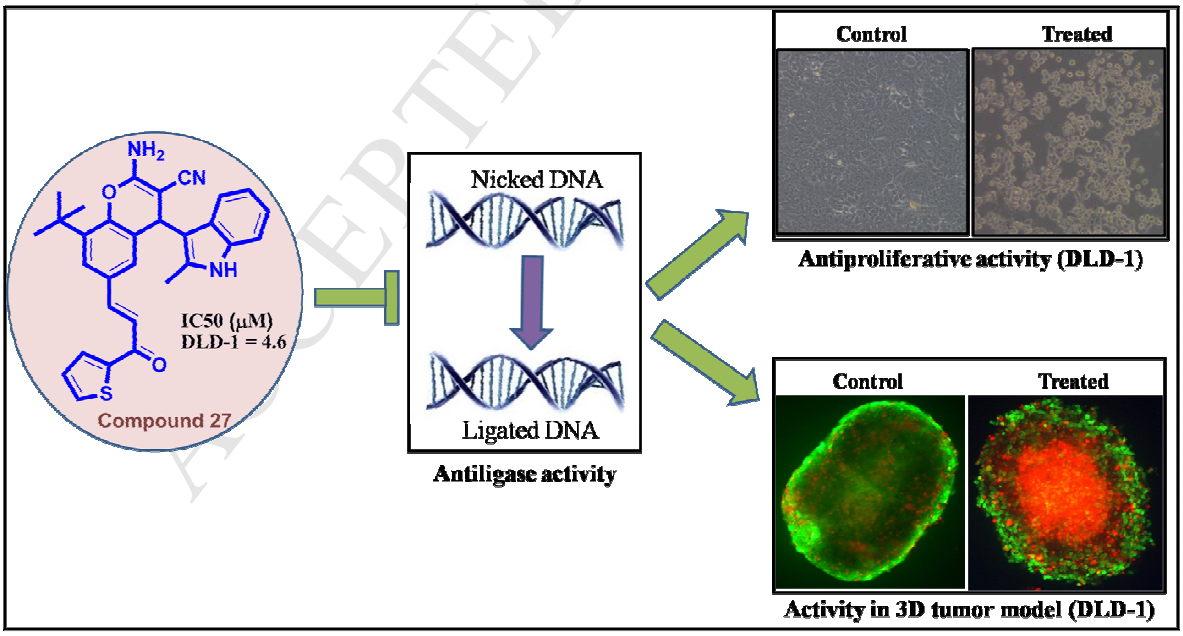

ACCEPTED MANUSCRIPT

Synthesis and bio-evaluation of indole-chalcone based benzopyrans as promising antiligase and antiproliferative agents

Sampa Gupta[1†], Pooja Maurya[2†], Akanksha Upadhyay[1], Pragati Kushwaha[1], Shagun Krishna[2], Mohammad Imran Siddiqi[2#], Koneni V. Sashidhara*[1#], Dibyendu Banerjee*[2#]

[1]Medicinal and Process Chemistry Division, [2]Molecular and structural biology division,

Academy of Scientific and Innovative Research (AcSIR), India

† Both authors contributed equally to this work.

CSIR-Central Drug Research Institute, (CSIR-CDRI), BS-10/1, Sector 10, Jankipuram Extension, Sitapur Road, Lucknow, 226031, India.

*Correspondence and requests for materials should be addressed to D.B (d.banerjee@cdri.res.in, dibyenducdri@gmail.com) and K.V.S (e-mail: sashidhar123@gmail.com, kv_sashidhara@cdri.res.in)

ABSTRACT

DNA replication and repair are complex processes accomplished by the concerted action of a network of enzymes and proteins. DNA ligases play a crucial role in these processes by catalyzing the nick joining between DNA strands. As compared to normal cells, elevated levels of human DNA ligase I (hLigI) is reported in some cancers. We studied the inhibition of hLigI mediated DNA nick sealing activity followed by the antiproliferative activity of novel indole-chalcone based benzopyran compounds on cancer cells. One molecule called compound **27** showed a notable preference for inhibition of hLigI as compared to other ligases and showed enhanced cytotoxicity against colon cancer (DLD-1) cells as compared to normal cells. Mechanistic studies showed that compound **27** directly interacts with hLigI in a competitive manner and did not interact with the DNA substrate during ligation. This novel and potent hLigI inhibitor showed significant inhibition of both monolayer culture as well as 3D culture of DLD-1 cells that mimic solid tumor. It also affected the migration of DLD-1 cells indicating the potential anti-metastatic activity. This novel hLigI inhibitor could therefore serve as a promising lead for anticancer drug development.

Keywords: Indole-chalcone based benzopyrans, DNA ligases, 3D culture, antiligase activity, antiproliferative activity

Abbreviations Used

BER (base excision repair), NER (nucleotide excision repair), HR (homologous recombination), NHEJ (non-homologous end joining), MMR (mismatch repair), TLS (translesion synthesis), FA (Fanconi anemia), MGMT (O^6 -methylguanine DNA methyltransferase), hLigI (human DNA ligase I), hLigIIIβ (human DNA ligase III), hLigIV (human DNA ligase IV), EMSA (Electrophoretic mobility shift assay) FDA (Fluorescein diacetate), PI (Propidium iodide).

ACCEPTED MANUSCRIPT

1. Introduction

The prime objective of each living organism is to transfer its hereditary material, intact and unaltered, to the next generation [1]. DNA replication and repair are essential molecular mechanisms required for error-free transfer of genetic material to the new generation, using a network of enzymes and proteins [2, 3, 4]. Errors in the replication, repair and recombination of DNA are reasons for genomic instability that can lead to unregulated cellular multiplication and cancer [5, 6, 7, 8]. Several DNA repair pathways are present inside the cells to cope with different genetic lesions [9, 10]. Cancer cells often have a slightly different set of DNA repair pathways from normal cells, to help them propagate despite errors in their DNA [11]. We therefore hypothesize that it might be a good strategy to target DNA repair proteins for cancer therapy; specially those proteins that are differentially expressed in cancer cells. Incidentally, the expression of hLigI has been reported to be elevated in several cancers like breast, lung and ovarian cancer cells, as compared to normal cells [12, 13]. DNA ligases have a crucial role in DNA replication and repair. They catalyze the joining of nicks by the formation of phosphodiester bonds between two adjacent DNA strands [14]. There are three types of ligases in mammalian cells, viz, ligase I (hLigI), ligase III (hLigIIIβ) and ligase IV (hLigIV) [15]. Human DNA ligase I is responsible for joining of Okazaki fragments during the lagging strand synthesis and involved in several DNA repair pathways such as NER (by hLigI and hLigIII) [16], BER (by hLigI and hLigIII) [17, 18] and microhomology-mediated end joining (by hLigI and hLigIII) [19, 20] whereas NHEJ is mediated by hLigIV [21]. In this manner, DNA ligation is a crucial requirement for all cells during replication and repair [22, 23, 24].

Inhibiting DNA ligases in cancer cell is shown to impede cell growth due to the accumulation of DNA strand breaks and lead to apoptotic cell death [13, 25]. In the past, several compounds were identified that can impede DNA nick sealing by inhibiting DNA ligases [4,

14, 20, 26, 27]; however, none of the inhibitors were potent enough to reach clinical trials on their own. Hence, there is a need for identification and characterization of more potent molecules. In order to find suitable DNA ligase inhibitors we searched the literature which suggested that indoles and their derivatives are highly versatile and common nitrogen-based heterocycles that are frequently used in the synthesis of important FDA approved anticancer drugs [28]. Indoles have recently attracted interest in anticancer research due to activity against several cancer cells. They are reported as potent inducers of apoptosis through a novel cell-based HTS caspase assay [29]. Singh *et al* have also reported indoles as highly promising anti-cancerous agents. They found that indole derivatives show appreciable inhibition of tumor growth in different cancer cell lines [30]. On the other hand, chalcones have attracted attention due to their wide range of potential biological activities [31, 32, 33, 34]. Rawat *et al* showed chalcone-resveratrol as a promising anticancer agent with selectivity towards certain ovarian, lung and breast cancer cell lines [35]. Our group has previously worked on chalcones and reported coumarin-chalcone hybrids as anticancer agents against four human cancer cell lines: KB (oral squamous cell carcinoma), C33A (cervical carcinoma), MCF-7 (breast adenocarcinoma) and A549 (lung cancer) [36]. Another pharmacophore with anticancer property is benzopyran. Recently, Sui *et al* showed benzopyrans as novel anticancer agents having an EC50 value of 2 nM [37]. William Kemnitzer *et al* demonstrated benzopyrans as potent caspase cascade activators and inducers of apoptosis in solid tumors [38]. Based on our long experience of working on molecular hybridization techniques [39], we designed a novel series of hybrid compounds in order to identify molecules that can inhibit DNA ligation and cell proliferation, and may serve as drug-like molecules. The design for this series is schematically represented in **scheme A** (figure 1). The molecules were synthesized and tested for their antiligase and antiproliferative activities in cancer cells. Finally, a detailed study of

the most active compound was carried out in order to verify the mode of action and cytotoxicity in *in vitro* and 3D tumor models.

2. Results and Discussion

2.1 Chemistry

The synthetic strategy of indole-chalcone based benzopyran molecules is depicted in scheme 1. In the first step, the Duff formylation on *ortho* substituted phenol (**1**-**4**) was carried out in the presence of HMTA with TFA as solvent at 120^{o} C for 4h followed by acid hydrolysis with 10% H_2SO_4 which gave aromatic dicarbaldehydes (**5**-**8**) [40]. The regioselective chalcones (**9**-**16**) were prepared from these dicarbaldehydes by reacting them with *para*-substituted acetophenones in the presence of conc. HCl as catalyst in dioxane [36]. Several research groups have worked upon multicomponent reactions taking salicylaldehyde, indole and different neucleophiles as reactive components in different reaction conditions to give benzopyran hybrids [41, 42, 43]. In a similar strategy, we carried out multicomponent reactions with chalcone intermediates, malononitrile (as neucleophile) and substituted 2-methyl indole in the presence of L-proline as catalyst in acetonitrile to give our target compounds (**17**-**29**) in quantitative yields. The reaction conditions were optimized for the choice of catalyst and the solvent. The structures of all the synthesized compounds were characterized with the help of ^{1}H and ^{13}C NMR spectral analysis coupled with mass spectrometry, which were in good agreement with the proposed structures (Supporting Information).

2.2. Inhibition of human DNA ligase I activity and cytotoxicity of synthesized compounds

The nick sealing activity of thirteen indole-chalcone based benzopyrans were determined for purified hLigI protein by gel-based, fluorescence-labelled DNA-ligation assays at 10 μM concentration as shown in figure 2. Among these thirteen compounds, four compounds (**20**,

23, **26** and **27**) showed >50% inhibition, two compounds (**22** and **28**) showed >45% inhibition, and other seven compounds showed <20% inhibition of nick sealing activity. All thirteen compounds were tested for their cytotoxic effect on various cancer cell lines viz. MDA-MB-231 (breast cancer), DLD-1 (colon cancer), HeLa (cervical cancer), HepG2 (liver cancer) and 4T1 (mouse breast cancer cell line) at 10 μM concentrations. The % inhibition of cancer cell proliferation by indole-chalcone based benzopyrans is represented in figure 3. Among them, five compounds (**24**, **25**, **27**, **28** and **29**) showed robust antiproliferative activity against tested cancer cell lines.

We found one compound which contains both thiazole and *tert*-butyl group in it (compound **27**) which possesses both antiligase (69.42 ± 3.05 % inhibition of nick sealing activity) and antiproliferative activity in various cancerous cell lines as depicted in figure 2 and 3. The IC_{50} values of compound **27** were calculated in various cancerous cell lines like MDA-MB-231, DLD-1, HeLa, HepG2 and 4T1 (IC_{50}<10 μM) from three independent experiments and plotted with the help of GraphPad Prism software version 5 (San Diego California USA). Compound **27** showed maximum antiproliferative activity against DLD-1 cells (IC_{50} = 4.6 μM). When further checked for cytotoxicity against the normal cell line HEK-293, we observed a three-fold lower cytotoxicity (IC_{50} = 12.4 μM) as shown in figure 4. Therefore, we selected compound **27** for detailed studies of mechanism of action.

2.3 Structure activity relationship (SAR) studies

From the available biological activity results and the diverse chemical structures of synthesized compounds, a preliminary structure activity relationship (SAR) was established. We found that the compounds showing > 50% inhibition in DNA ligation assay mainly contained *tert*-butyl and NH_2 group at C-8 and C-2 positions of benzopyran rings, respectively. In addition, the imperative role of these substituents was supported in docking studies. Further, substitution in the indole ring did not bring significant effect in inhibition of

hLigI activity. Moreover, when some of the structures were modified by replacing aryl group from chalcone with a thiazole moiety, they showed marked cytotoxic activity towards various cancer cell lines. Preliminary SAR analysis revealed that *tert*-butyl, amino and thiazole moieties are essential for inhibition of DNA nick sealing activity of hLigI and for cytotoxic activity against cancer cell lines. This was most evident in compound **27,** which emerged as the potential lead. The SAR is summarized in a pictorial diagram in figure 5.

2.4 Specific activity of compound **27** *against various ATP-dependent DNA ligases*

For determination of specific activity against various ATP-dependent DNA ligases, we performed a DNA nick-sealing assay in a concentration dependent manner against three different human DNA ligases viz., hLigI, hLigIIIβ, and hLigIV/XRCC4 and the non-human T4 DNA ligase. We found that compound **27** inhibited hLigI in a concentration dependent manner, with some overlapping activity against hligIV/XRCC4; however, the compound was completely inactive against hligIIIβ and T4 DNA ligase as shown in figure 6. Hence, this compound specifically inhibits the activity of hligI with some overlapping activity against hligIV/XRCC4 as depicted in figure 6.

2.5 Interaction study of compound ***27*** *with hLigI and DNA*

DNA ligation activity in the presence of compound **27** can be inhibited in two ways, either by direct interaction with human DNA ligase I or by interaction with the DNA to indirectly obstruct protein binding. To study the interaction of compound **27** with both protein and DNA, we performed *in silico* molecular docking followed by gel electrophoretic mobility shift assay (EMSA) and DNase I cleavage protection assay. *In silico* docking of compound **27** into the DNA binding site of hLigI (PDB ID-1X9N) showed that the compound binds to hLigI with a predicted binding energy of -14.66 kJ/mole (Figure 7). As seen in figure 7, one

hydrogen atom of amino group attached with a chromene ring forms a hydrogen bond with Lys770, while a second hydrogen atom interacts with Gly773. Further, a hydrogen bond was observed with Arg451. Two of these residues (Lys770 and Arg451) are involved in direct hydrogen bond formation with DNA in the crystal structure and are therefore, anticipated to have a significant effect on the binding of hLigI with DNA [26, 44 and 45]. Therefore, these interactions of compound **27** with hLigI play an important role in the stability of the docked complex; further, the interaction of these amino acid residues with compound **27** can explain the potent hLigI inhibition observed in the *in vitro* assays.

In the EMSA study, we observed a significantly reduced interaction between hLigI and DNA in the presence of increasing concentrations of compound **27** (31.25, 62.5, 125, 250 and 500 μM), indicating that compound **27** interacts with hLigI by replacing the interacting DNA substrate, as shown in figure 8. Thus, hLigI was inhibited by a competitive mode of inhibition.

DNase I cleavage protection assay showed that unlike DNA interacting molecules such as doxorubicin (DNA intercalator), DAPI (DNA minor grove binder) and methyl green (DNA major groove binder); there was a complete cleavage of DNA in the presence of ampicillin (negative control) and compound **27** (at 250, 500 and 700μM concentrations), even at very high concentrations. This suggested that compound **27** does interact with DNA either through intercalation or through DNA minor/ major groove binding. Therefore, DNA incubated with compound 27 was left free for cleavage by DNase I (figure 9).

*2.6 Compound **27** induces morphological changes in DLD-1 cells*

We studied the morphological changes in DLD-1 cells induced by compound **27**. The bright field images of DLD-1 cells showed significant morphological changes after 24 and 48 h of treatment with compound **27** at 5 and 10 μM concentrations, as compared to the control cells

(figure 10). The observed morphological changes were shrinkage of cells and detachment of cells from the culture surface that are the characteristic of cells undergoing apoptosis. We observed that in the presence of compound **27,** the cells undergo apoptosis in a concentration and time dependent manner (figure 10).

*2.7 Compound **27** inhibits colony formation in DLD-1 cell line*

The colony-forming assay determines the ability of a cell to proliferate indefinitely, thereby retaining its reproductive ability to form a colony or a clone. Colony formation by DLD-1 cells was observed by staining with crystal violet. DLD-1 cells were treated with compound **27** (at 1.25, 2.5 and 5 μM concentrations) for 24 h and 48 h and cell colonies were grown for 10 days before staining. Figure 11 confirms inhibition of colony formation in the presence of compound **27** in a time and concentration dependent manner.

*2.8 Compound **27** inhibits migration of colon cancer cells*

Cell migration is a highly coordinated and multi-step process that plays a critical role in progression of cancer. Cancer cells often have a highly metastatic nature. Wound-healing assay is a simple and inexpensive method to study the directional migration of cells *in vitro* [46]. Thus, we studied the effects of compound **27** on the migration of colon cancer cells by wound-healing assay in DLD-1 cells, after treatment with different concentrations of the compound (2.5 and 5 μM) for 12, 24 and 48 h. Percentage open area in untreated and treated cells were calculated at different time points with the help of Image-J software. The bright field images and graphs represented in figure 12 showed a significant reduction in % open area of control cells as compared to treated cells. Decrease in % open area indicates increased migration. Therefore, we determined that compound **27** could significantly inhibit cellular migration at 2.5 and 5 μM concentrations suggesting that it might have anti-metastatic activity against colon cancer cells.

*2.9 Compound **27** induces apoptosis in DLD-1 cells*

In order to check the effect of compound **27** on cellular apoptosis, DLD-1 cells were exposed to different concentrations of compound **27** for 48 h, and stained with Annexin V-FITC and PI. Flow cytometry analysis of stained cells showed the induction of apoptosis in DLD-1 cells in a dose dependent manner (2.5, 5 and 10μM). At 5 μM concentration 17.38 ± 2.23 % cells were in early apoptosis and 14.85 ± 2.18 % cells in late apoptosis whereas at 10 μM concentration percentage of early and late apoptotic cells increased upto 26.53 ± 1.51% and 50.96 ± 6.98% respectively, as shown in figure 13. Hence, the induction of apoptosis was responsible for death of DLD-1 cells after treatment with compound **27**.

*2.10 Effect of compound **27** on DLD-1 3D spheroids imitating solid tumors*

3D spheroids are good mimics of *in vivo* tumor system in *in vitro* study and provide physiologically more relevant information than 2D cultures [47]. In previous experiments, we checked the effectiveness of compound **27** against DLD-1 cells in 2D culture. Thereafter, in order to investigate the potential effect of compound **27** on solid tumors, we developed 3D-spheroids of DLD-1 cells and treated them with compound **27** for 72 h, followed by live dead staining with FDA and PI. The dye FDA produces green fluorescence when it enters the viable cells whereas PI, the nuclear staining dye cannot pass through the cell membrane of viable cells but can enter dead cells via the disordered membranes and stains the nuclear DNA to produce red fluorescence. In control spheroids, there was significantly less number of dead cells as compared to cells treated with increasing concentrations of compound **27** (6.25, 12.5 and 25μM). In contrast, the spheroids treated with compound **27** showed increased cell death with a distinct necrotic center after 72 h of treatment, highlighted by the increased red fluorescence visible in figure 14. More dead cells appear at the center because

of lower levels of nutrients and oxygen supply and increased level of debris, CO_2, and acidosis, as compared to cells present at the periphery [48].

3. Conclusions

In this study, we identified a novel hLigI inhibitor (compound **27**) that induced antiproliferative activity against cancer cell lines (DLD-1, MDA-MB-231, HeLa, HepG2 and 4T1), but most prominently targeted the colon cancer cell line DLD-1 (Figure 3). The compound specifically inhibited hLigI mediated nick sealing activity in a competitive manner by interacting with the DNA binding residues of the protein (Figure 7 & 8). Compound **27** inhibited the migration of DLD-1 cells suggesting a potential anti-metastatic activity (Figure 12). Compound **27** induced apoptosis in monolayer cultures and more interestingly, was effective against 3D-spheroids of DLD-1 cells that resembled solid tumors. Therefore, this novel class of hLigI inhibitor is a promising lead for drug development for colorectal cancer. The impact of ligase inhibitors in combination with radiation and DNA damaging chemotherapeutic agents is a subject of further research in our laboratory.

4. Experimental Section

4.1. General Procedure: All chemical reagents were procured commercially and used without further purification. Column chromatography was carried out on silica gel (60-120 and 100-200 mesh). All reactions were monitored by TLC (silica gel plates with fluorescence F254). Melting points were uncorrected. The ^{1}H and ^{13}C NMR spectra were recorded on 400, 500 MHz and 100, 125 MHz, respectively, using DMSO- d_6 as solvents and TMS as internal standard. All chemical shifts values were given in ppm and their multiplicities expressed as: s = singlet, brs = broad singlet, d = doublet, brd = broad doublet, dd = double doublet, t = triplet, q = quartet, m = multiplet. IR spectra were recorded in the range of 500 ~ 4000 cm^{-1}. High performance liquid chromatography analyses for checking purity of targeted

compounds were performed on Waters 2998, and detection was done by UV detector. All final compounds were found to be >95% pure by HPLC (Supporting Information).

4.2. General synthetic procedure for the preparation of 4-Hydroxy-5-alkyl isophthalaldehydes (**5-8**).

2-Alkyl phenol (1.0 equiv.) and hexamethylenetetramine (HMTA) (1.2 equiv.) were dissolved in TFA (25 mL) and the solution was heated at 120 ºC for 3 h. After cooling to room temperature, 10 % aq.H_2SO_4 (25 mL) was added and the temperature maintained at 90-100 ºC for two more hours. The solution was basified with $NaHCO_3$ to pH=8 and extracted with $CHCl_3$ (50 mL x 3). The combined organic layers were dried over anhy. Na_2SO_4, filtered, and concentrated to dryness under reduced pressure. The crude product thus obtained was purified on a silica gel column (100-200 mesh) using ethylacetate-hexane (12:88, v/v) as eluent to afford compounds **5-8** in good yields [39].

4.3. General synthetic procedure for preparation of compounds (**9-16)**

A solution of 4-hydroxy-5-alkyl isophthalaldehyde **5-8** (1.0 equiv.) and 4-substituted acetophenone (1.0 equiv.) in dioxane (15 mL) was treated with conc. HCl (2 mL). The resultant solution was refluxed for 8-10 h. After completion of the reaction as checked by TLC, the reaction mixture was cooled and the excess dioxane was removed under reduced pressure. The residue thus obtained was suspended in water (50 mL) and extracted 3-fold with $CHCl_3$ (50 mL). The combined organic layers were dried on anhydrous Na_2SO_4, filtered, and concentrated to dryness under reduced pressure. The residue was purified by silica gel (230-400 mesh) column chromatography using ethyl acetate-hexane (10:90, v/v) as eluent to afford regioselective parachalcones **9-16** in moderate yields [49].

*4.4. General procedure for the synthesis of compounds (**17-29**)*

Para substituted chalcones (1 equiv.) (**9**-**16**) and malononitrile (1 equiv.) were stirred in acetonitrile in the presence of L-proline catalyst at room temperature for half an hour. To this reaction mixture different 2-methyl indole (0.8 equiv.) were added and was heated to 90^{o} C on an oil bath. Reaction mixture was stirred till the completion of reaction as monitored by TLC. Afterwards, the reaction mixture was evaporated to dryness under vacumm and was partitioned between ethyl acetate and water. The combined organic layer was dried and purified by silica gel column chromatography to get pure products **17**-**29** [50].

(E)-2-amino-8-(tert-butyl)-4-(2-methyl-1H-indol-3-yl)-6-(3-oxo-3-(p-tolyl)prop-1-en-1-yl)-4H-chromene-3-carbonitrile (**17**).

Yellow solid, yield: 75%; mp: 193 ºC; ^{1}H NMR (DMSO-d_6, 400 MHz) δ: 1.51 (s, 9H), 2.39 (s, 3H), 2.51 (s, 3H), 5.04 (s, 1H), 6.76 (t, J = 7.9 Hz, 1H), 6.87 (s, 2H, NH_2), 6.92 (t, J = 7.9 Hz, 1H), 7.02 (d, J = 7.9 Hz, 1H), 7.22 (d, J = 8.1 Hz, 1H), 7.31 (s, 1H), 7.34 (d, J = 8.1 Hz, 2H), 7.56-7.60 (m, 3H), 7.96 (d, J = 8.2 Hz, 2H), 10.86 (s, 1H, NH); ^{13}C NMR (DMSO-d_6, 100 MHz) δ: 11.8 (CH_3 of indole), 21.6 (CH_3 of Ph), 30.4 (CH_3 of ^{t}*Bu*), 31.9 (CH of pyran), 35.2 ($\underline{C}(CH_3)_3$), 56.7 ($\underline{C}$-CN), 111.2, 115.1, 117.7, 118.8, 120.5, 121.1 (Ar), 121.7, 125.1 (CN), 125.7, 126.7, 128.9, 129.1, 129.7, 130.5, 132.4, 135.5, 135.9, 137.8 (Ar), 143.8, 143.9, 149.6 (Ar), 159.4 (C-NH_2), 189.1(C=O); ESI-MS (*m/z*): 502.1 $(M+H)^{+}$; HRMS *m/z* calcd for $C_{33}H_{31}N_3O_2$ $(M+H)^{+}$ 502.2495, found 502.2491.

(E)-2-amino-8-(tert-butyl)-6-(3-(4-methoxyphenyl)-3-oxoprop-1-en-1-yl)-4-(2-methyl-1H-indol-3-yl)-4H-chromene-3-carbonitrile(**18**).

Yellow solid, yield: 78%; mp: 190 ºC; ^{1}H NMR (DMSO-d_6, 400 MHz) δ: 1.49 (s, 9H), 2.50 (s, 3H), 3.80 (s, 3H), 5.03 (s, 1H), 6.76 (t, J = 7.4 Hz, 1H), 6.89 (s, 2H, NH_2), 6.91 (t, J = 7.5 Hz, 1H), 7.01(d, J = 8.2 Hz, 3H), 7.21 (d, J = 8.0 Hz, 1H), 7.28 (brs, 1H), 7.50 (d, J = 15.6 Hz, 1H), 7.54 (s, 1H), 7.60 (d, J = 15.6 Hz, 1H), 8.04 (d, J = 8.7 Hz, 2H), 10.84 (s, 1H, NH); ^{13}C NMR (DMSO-d_6, 100 MHz) δ:11.8 (CH_3), 30.1 (CH_3 of ^{t}*Bu*), 31.6 (CH of pyran), 35.0

(C(CH$_3$)$_3$), 55.5 (OCH$_3$), 60.8 (C-CN), 110.6 , 113.8, 114.2, 117.9, 119.4, 119.8, 121.2 (Ar), 121.4, 124.0, 125.5, 126.8, 128.1, 130.8, 131.0, 131.1, 131.9, 135.5, 137.6 (Ar) 143.5, 149.2 (Ar-O), 158.1 (C-NH$_2$), 163.4 (Ar-OMe), 188.9 (C=O); ESI-MS (*m/z*): 518.2 $(M+H)^+$; HRMS *m/z* calcd for $C_{33}H_{31}N_3O_3$ $(M+H)^+$ 518.2444, found 518.2442.

(E)-2-amino-8-(tert-butyl)-4-(2-methyl-1H-indol-3-yl)-6-(3-oxo-3-(3, 4, 5-trimethoxyphenyl) prop-1-en-1-yl)-4H-chromene-3-carbonitrile(**19**).

Yellow solid, yield: 75%; mp: 147 ºC; ^{1}H NMR (DMSO-d_6, 500 MHz) δ: 1.50 (s, 9H), 2.51 (s, 3H), 3.75 (s, 3H), 3.86 (s, 3H), 5.05 (s, 1H), 6.76 (t, *J* = 7.6 Hz, 1H), 6.88 (s, 2H, NH$_2$), 6.92 (t, *J* = 7.8 Hz, 1H), 7.03 (d, *J* = 8.2 Hz, 1H), 7.22 (d, *J* = 8.1 Hz, 1H), 7.31 (s, 2H), 7.34 (s, 1H), 7.56-7.59 (m, 3H), 10.86 (s, 1H, NH); ^{13}C NMR (DMSO-d_6, 100 MHz) δ: 11.7 (CH$_3$), 30.3 (CH$_3$ of ^{t}*Bu*), 31.8 (CH of pyran), 35.1 (C(CH$_3$)$_3$), 56.6 (OCH$_3$), 60.6 (C-CN), 106.6, 111.2, 115.0, 117.7, 118.8, 120.5, 121.1 (Ar), 121.8, 125.2 (CN), 126.1, 126.7, 128.6, 130.5, 132.4, 133.5, 135.8, 137.8 142.3, 143.9 (Ar), 149.6 (Ar-O), 153.3(Ar-OMe), 159.5(C-NH$_2$), 188.5(C=O); ESI-MS (*m/z*): 578.1 $(M+H)^+$; HRMS *m/z* calcd for $C_{35}H_{35}N_3O_5$ $(M+H)^+$ 578.2655, found 578.2649.

(E)-2-amino-8-(tert-butyl)-6-(3-(4-chlorophenyl)-3-oxoprop-1-en-1-yl)-4-(2-methyl-1H-indol-3-yl)-4H-chromene-3-carbonitrile (**20**).

Yellow solid, yield: 77%; mp: 157 ºC ^{1}H NMR (DMSO-d_6, 400 MHz) δ: 1.51 (s, 9H), 2.51 (s, 3H), 5.04 (s, 1H), 6.76 (t, *J* = 7.5 Hz, 1H), 6.87 (s, 2H, NH$_2$), 6.92 (t, *J* = 7.4 Hz, 1H), 7.01 (d, *J* = 7.9 Hz, 1H), 7.22 (d, *J* = 7.9 Hz, 1H), 7.32 (s, 1H), 7.59-7.61 (m, 5H), 8.07 (d, *J* = 8.6 Hz, 2H), 10.86 (s, 1H, NH); ^{13}C NMR (DMSO-d_6, 100 MHz) δ: 11.8 (CH$_3$), 30.4 (CH$_3$ of ^{t}*Bu*), 31.9 (CH of pyran), 35.2 (C(CH$_3$)$_3$), 56.7 (C-CN), 111.2, 115.0, 117.7, 118.8, 120.5, 121.0, 121.4, 125.1, 125.9, 126.7, 129.1, 129.3, 130.4, 130.9, 132.4, 135.9, 136.7, 137.8, 138.3, 144.7 (Ar), 149.8 (Ar-O), 159.4 (C-NH$_2$), 188.7 (C=O); ESI-MS (*m/z*): 522.0 $(M+H)^+$; HRMS *m/z* calcd for $C_{32}H_{28}ClN_3O_2$ $(M+H)^+$ 522.1948, found 522.1948.

(E)-2-amino-8-(sec-butyl)-4-(2-methyl-1H-indol-3-yl)-6-(3-oxo-3-(3, 4, 5-trimethoxyphenyl) prop-1-en-1-yl)-4H-chromene-3-carbonitrile (**21**).

Yellow solid, yield: 70%; mp: 220 ºC; ^{1}H NMR ($CDCl_3$, 400 MHz) δ: 0.93-0.97 (m, 3H), 1.34 (dd, J_1 = 4.6Hz, J_2 = 2.3Hz, 3H), 1.69-1.74 (m, 2H), 2.49 (s, 3H), 3.17-3.25 (m, 1H), 3.89 (s, 6H), 3.94 (s, 3H), 4.66 (s, 2H), 5.14 (s, 1H), 6.90-6.95 (m, 1H), 7.05-7.19 (m, 6H), 7.25-7.28 (m, 1H), 7.33 (s, 1H), 7.56 (t, J = 15.7Hz, 1H), 8.09 (s, 1H, NH); ^{13}C NMR ($CDCl_3$, 100 MHz) δ:11.8 (CH_3), 12.1, 20.6, 30.3, 31.6, 33.7, 56.4, 60.7, 60.9 (Aliphatic), 106.2, 110.6, 113.9, 117.9, 119.4, 121.1, 121.5, 123.4, 125.8, 126.9, 127.5, 131.3, 132.1, 133.5, 135.3, 135.5, 142.4, 144.2, 148.1, 153.1, 158.6 (C-NH_2), 189.7 (C=O); ESI-MS (*m/z*): 578.1 $(M+H)^+$; HRMS *m/z* calcd for $C_{35}H_{35}N_3O_5$ $(M+H)^+$ 578.2655, found 578.2660.

(E)-2-amino-8-(tert-butyl)-4-(5-methoxy-2-methyl-1H-indol-3-yl)-6-(3-oxo-3-(p-tolyl)prop-1-en-1-yl)-4H-chromene-3-carbonitrile(**22**).

Yellow solid, yield: 72%; mp: 163 ºC; ^{1}H NMR (DMSO-d_6, 400 MHz) δ: 1.51 (s, 9H), 2.39 (s, 3H), 2.51 (s, 3H), 3.60 (s, 3H), 5.00 (s, 1H), 6.53 (s, 1H), 6.58 (dd, J_1 = 6.2Hz, J_1 = 2.4Hz, 1H), 6.89 (s, 2H, NH_2), 7.11 (d, J = 8.7Hz, 1H), 7.34 (d, J = 8.1Hz, 3H), 7.58-7.61 (m, 3H), 7.97 (d, J = 8.2Hz, 2H), 10.69 (s, 1H,NH); ^{13}C NMR (DMSO-d_6, 100 MHz) δ:11.9 (CH_3), 21.6, 30.4, 31.9, 35.2, 55.5, 56.5 (Aliphatic), 100.2, 109.9, 111.7, 115.0, 121.1, 121.7, 125.1, 125.7, 127.0, 128.9, 129.1, 130.6, 130.9, 133.1, 135.5, 137.9, 143.9, 149.5, 153.2, 159.6 (C-NH_2), 189.2 (C=O); ESI-MS (*m/z*): 532.1 $(M+H)^+$; HRMS *m/z* calcd for $C_{34}H_{33}N_3O_3$ $(M+H)^+$ 532.2600, found 532.2602.

(E)-2-amino-8-(tert-butyl)-4-(5-chloro-2-methyl-1H-indol-3-yl)-6-(3-oxo-3-(p-tolyl)prop-1-en-1-yl)-4H-chromene-3-carbonitrile (**23**).

Yellow solid, yield: 75%; mp: 175 ºC; ^{1}H NMR (DMSO-d_6, 400 MHz) δ: 1.52 (s, 9H), 2.38 (s, 3H), 2.53 (s, 3H), 5.03 (s, 1H), 6.91-6.96 (m, 4H), 7.23 (d, J = 8.4 Hz, 1H), 7.34 (d, J = 8.0 Hz, 3H), 7.56 (d, J = 15.6Hz, 1H), 7.60 (s, 1H), 7.64 (d, J = 15.7Hz, 1H), 7.97 (d, J = 8.1

Hz, 2H), 11.09 (s, 1H, NH); ^{13}C NMR (DMSO-d_6, 100 MHz) δ:11.8 (CH_3), 21.6, 30.4, 31.8, 35.2, 56.4, 79.6 (Aliphatic), 112.6, 115.3, 116.9, 120.3, 120.9, 121.8, 123.5, 124.7, 125.9, 127.7, 128.9, 129.1, 129.7, 130.7, 134.3, 135.5, 137.9, 143.7, 143.8, 149.6, 159.4 (C-NH_2), 189.1 (C=O); ESI-MS (*m/z*): 536.2 $(M+H)^+$; HRMS *m/z* calcd for $C_{33}H_{30}ClN_3O_2$ $(M+H)^+$ 536.2105, found 536.2109.

(E)-2-amino-8-isopropyl-4-(2-methyl-1H-indol-3-yl)-6-(3-oxo-3-(thiophen-2-yl)prop-1-en-1-yl)-4H-chromene-3-carbonitrile (**24**).

Yellow solid, yield: 70%; mp: 183 ºC; ^{1}H NMR (DMSO-d_6, 400 MHz) δ: 1.32-1.35 (m, 6H), 2.52 (s, 3H), 3.46-3.53 (m, 1H), 5.05 (s, 1H), 6.77 (t, J = 7.3 Hz, 1H), 6.84 (s, 2H, NH_2), 6.93 (t, J = 7.3Hz, 1H), 6.99 (d, J = 7.9Hz, 1H), 7.23 (d, J = 7.9Hz, 2H), 7.28 (t, J = 4.7Hz, 1H), 7.54 (d, J = 15.6 Hz, 1H), 7.64 (d, J = 15.6Hz, 1H), 7.72 (s, 1H), 8.02 (d, J = 4.3Hz, 1H), 8.26 (d, J = 3.3 Hz, 1H), 10.86 (s, 1H,NH); ^{13}C NMR (DMSO-d_6, 100 MHz) δ:11.8 (CH_3), 22.8, 23.4, 26.9, 31.8, 56.8 (Aliphatic), 111.2, 114.7, 117.7, 118.8, 120.5, 121.1, 121.3, 124.4, 125.1, 126.8, 129.0, 129.2, 130.8, 132.5, 134.1, 135.8, 135.9, 136.5, 143.2, 145.9, 148.1, 159.9 (C-NH_2), 181.9 (C=O).; ESI-MS (*m/z*): 480.1 $(M+H)^+$; HRMS *m/z* calcd for $C_{29}H_{25}N_3O_2S$ $(M+H)^+$ 480.1746, found 480.1748.

(E)-2-amino-8-isopropyl-4-(5-methoxy-2-methyl-1H-indol-3-yl)-6-(3-oxo-3-(thiophen-2-yl)prop-1-en-1-yl)-4H-chromene-3-carbonitrile (**25**).

Light yellow solid, yield: 72%;mp: 156 ºC; ^{1}H NMR (DMSO-d_6, 400 MHz) δ: 1.32-1.36 (m, 6H), 2.50 (s, 3H), 3.44-3.51 (m, 1H), 3.60 (s, 3H), 5.01 (s, 1H), 6.49 (d, J = 2.3Hz, 1H), 6.58 (dd, J_1 = 6.2Hz, J_2 =2.4Hz, 1H), 6.86 (s, 2H), 7.11 (d, J = 8.7Hz, 1H), 7.25 (s, 1H), 7.28-7.31 (m, 1H), 7.54-7.68 (m, 2H), 7.72 (s, 2H), 8.03 (dd, J_1 = 3.9Hz, J_2 =1.0Hz, 1H), 8.27 (dd, J_1 = 2.8Hz, J_2 =1.0Hz, 1H), 10.69 (s, 1H, NH); ^{13}C NMR (DMSO-d_6, 125 MHz) δ:11.9 (CH_3), 22.8, 23.4, 27.2, 31.9, 55.4, 56.7 (Aliphatic), 100.5, 109.7, 111.7, 114.7, 121.1, 121.4, 124.4, 125.2, 127.1, 129.0, 129.2, 130.8, 130.9, 133.2, 134.0, 135.8, 136.4, 143.2, 145.9, 148.2,

153.2, 159.9 (C-NH_2), 181.9 (C=O).; ESI-MS (*m/z*): 510.0 $(M+H)^+$; HRMS *m/z* calcd for $C_{30}H_{27}N_3O_3S$ $(M+H)^+$ 510.1851, found 510.1847.

(E)-2-amino-8-(tert-butyl)-4-(5-chloro-2-methyl-1H-indol-3-yl)-6-(3-(4-methoxyphenyl)-3-oxoprop-1-en-1-yl)-4H-chromene-3-carbonitrile (**26**).

Light yellow solid, yield: 72%;mp: 202 ºC; ^{1}H NMR (DMSO-d_6, 400 MHz) δ: 1.51 (s, 9H), 2.52 (s, 3H), 3.84 (s, 3H), 5.02 (s, 1H), 6.92-6.93 (m, 4H), 7.04 (d, *J* = 8.5Hz, 2H), 7.22 (d, *J* = 8.4Hz, 1H), 7.33 (s, 1H), 7.53 (d, *J* = 15.6Hz, 1H), 7.58 (s, 1H), 7.64 (d, *J* = 15.6Hz, 1H), 8.06 (d, *J* = 8.4Hz, 2H), 11.09 (s, 1H); ^{13}C NMR (DMSO-d_6, 100 MHz) δ:11.8 (CH_3), 30.4, 31.8, 35.2, 55.9, 56.4 (Aliphatic), 112.7, 114.4, 115.3, 116.9, 120.4, 121.0, 121.8, 123.5, 124.7, 125.9, 127.7, 128.8, 130.8, 130.9, 131.4, 134.4, 137.9, 143.3, 149.5, 159.5 (C-NH_2), 163.6 (Ar-OMe), 187.9 (C=O).; ESI-MS (m/z): 536.1 $(M+H)^+$; HRMS m/z calcd for $C_{33}H_{30}ClN_3O_2$ $(M+H)^+$ 552.0626, found 552.2047.

(E)-2-amino-8-(tert-butyl)-4-(2-methyl-1H-indol-3-yl)-6-(3-oxo-3-(thiophen-2-yl)prop-1-en-1-yl)-4H-chromene-3-carbonitrile (**27**).

Light yellow solid, yield: 70%; mp: 208 ºC; ^{1}H NMR (DMSO-d_6, 400 MHz) δ: 1.52 (s, 9H), 2.52 (s, 3H), 5.05 (s, 1H), 6.76 (t, *J* = 7.2Hz, 1H), 6.88 (s, 2H), 6.92 (t, *J* = 7.1Hz, 1H), 7.02 (d, *J* = 8.0Hz, 1H), 7.23 (d, *J* = 8.0Hz, 1H), 7.28 (t, *J* = 4.6Hz, 1H), 7.32 (s, 1H), 7.58-7.60 (m, 3H), 8.01 (d, *J* = 4.3Hz, 1H), 8.24 (d, *J* = 3.4Hz, 1H), 10.86 (s, 1H); ^{13}C NMR (DMSO-d_6, 100 MHz) δ:11.8 (CH_3), 30.4, 31.9, 35.2, 56.7, 79.6 (Aliphatic), 111.2, 115.0, 117.7, 118.8, 120.5, 121.1, 121.3, 125.1, 125.9, 126.7, 129.0, 129.3, 130.3, 132.4, 134.1, 135.8, 137.9, 143.4, 145.8, 149.7, 159.4 (C-NH_2), 181.9 (C=O).; ESI-MS (*m/z*): 494.2 $(M+H)^+$; HRMS *m/z* calcd for $C_{30}H_{27}N_3O_2S$ $(M+H)^+$ 494.1902, found 494.1897.

(E)-2-amino-8-methyl-4-(2-methyl-1H-indol-3-yl)-6-(3-oxo-3-(thiophen-2-yl)prop-1-en-1-yl)-4H-chromene-3-carbonitrile (**28**).

Light yellow solid, yield: 72%;mp: 202 ºC; ^{1}H NMR (DMSO-d_6, 500 MHz) δ: 2.39 (s, 3H), 2.51 (s, 3H), 5.05 (s, 1H), 6.78 (t, J = 7.2Hz, 1H), 6.83 (s, 2H, NH_2), 6.93 (t, J = 7.8Hz, 1H), 6.97 (d, J = 8.1Hz, 1H), 7.17 (s, 1H), 7.23 (d, J = 8.0Hz, 1H), 7.28 (t, J = 4.0Hz, 1H), 7.50 (d, J = 15.5Hz, 1H), 7.62 (d, J = 15.5Hz, 1H), 7.73 (s, 1H), 8.02 (d, J = 4.9Hz, 1H), 8.22 (d, J = 3.7Hz, 1H), 10.87 (s, 1H, NH); ^{13}C NMR (DMSO-d_6, 100 MHz) δ:11.8 (CH_3), 15.9, 31.6, 56.9 (Aliphatic), 111.2, 114.4, 117.7, 118.8, 120.5, 121.1, 121.4, 124.1, 126.1, 126.8, 128.9, 129.3, 130.5, 132.7, 133.9, 135.8, 135.9, 142.9, 145.9, 149.1, 159.8 (C-NH_2), 181.9 (C=O).; ESI-MS (*m/z*): 452.0 $(M+H)^+$; HRMS *m/z* calcd for $C_{27}H_{21}N_3O_2S$ $(M+H)^+$ 452.1433, found 452.1432.

(E)-2-amino-8-(tert-butyl)-4-(5-methoxy-2-methyl-1H-indol-3-yl)-6-(3-oxo-3-(thiophen-2-yl)prop-1-en-1-yl)-4H-chromene-3-carbonitrile (**29**).

Light yellow solid, yield: 70%; mp: 209 ºC; ^{1}H NMR (DMSO-d_6, 400 MHz) δ: 1.51 (s, 9H), 2.52 (s, 3H), 3.60 (s, 3H), 5.00 (s, 1H), 6.52 (s, 1H), 6.58 (dd, J_1 = 6.5Hz, J_2 = 2.1Hz, 1H), 6.89 (s, 2H, NH_2), 7.11 (d, J = 8.6 Hz, 1H), 7.28 (t, J = 4.0Hz, 1H), 7.34 (s, 1H), 7.59 (s, 2H), 8.03 (d, J = 4.4Hz, 1H), 8.25 (d, J = 3.1Hz, 1H), 8.32 (s, 1H), 10.69 (s, 1H, NH); ^{13}C NMR (DMSO-d_6, 100 MHz) δ:11.9, 30.4, 31.9, 35.2, 55.5, 56.5, 79.6 (Aliphatic), 100.2, 109.9, 111.7, 115.0, 121.1, 121.4, 125.2, 125.9, 127.0, 129.2, 130.3, 130.9, 133.1, 134.1, 135.8, 137.9, 143.4, 145.8, 149.6, 153.2, 159.6 (C-NH_2), 181.9 (C=O).; ESI-MS (*m/z*): 524.3 $(M+H)^+$; HRMS *m/z* calcd for $C_{31}H_{29}N_3O_3S$ $(M+H)^+$ 524.2008, found 524.2004.

4.5. Biological Methods

4.5.1. In vitro DNA nick sealing (ligation) assay

DNA ligation assays were performed as previously described [26]. For the generation of linear duplex DNA ligase substrate, we used three different single strand DNA oligomers, 52-mer (5′-GTACGTCGATCGATTGGTAGATCAGTGTCTATGTATGTCAGTGAGATAGT

AC-3′), 25-mer (5′-CTGATCTACCAATCGATCGACGTAC-3′) and 27-mer (5′-/5Cy3/GTACTATCTCACTGACATACATAGACA-3′) and annealed them together to form a ds nicked DNA substrate for DNA ligase I nick sealing activity, in the presence of ATP. The reaction mixture (20 μL) contained 1 pmol of labeled DNA substrate and 0.2 pmol of purified hLigI in a ligation buffer containing Tris-Cl (50 mM, pH 7.5), MgCl2 (10 mM), BSA (0.25 mg/mL), NaCl (100 mM), and ATP (500 μM). The nicked duplex DNA was incubated with purified hLigI in the absence or presence of inhibitors at 37 °C for 30 min. After 30 min, 10 μL of stop buffer (90% formamide and 10% of 50 mM EDTA) was added to stop the reaction. This reaction mixture was loaded onto a denaturing gel containing 7 M urea and 12% acrylamide used for the separation of ligated and un-ligated DNA products. Ligated duplex DNA appeared higher in the gel due to the larger size, whereas un-ligated product would appear lower due to smaller size. If an inhibitor is added to the reaction mixture, this would lead to an inhibition of ligation and a corresponding loss of labelled ligated product in the gel. The percentage inhibition of ligation was estimated by measuring the density (by GE Image Quant LAS 4010) of ligated product in the lane without inhibitor and comparing it with the lanes containing different inhibitors or with the same inhibitor at different concentrations. Experiments were carried out in triplicate and average values are represented graphically.

4.5.2. Cell culture and viability assays

To determine whether the synthesized compounds could affect proliferation of cancer cells, various types of cancerous cell lines were cultured. The human breast cancer (MDA-MB-231) and hepatic cancer (HepG2) cell lines (ATCC, Manassas, VA) were grown in DMEM. Human cervical cancer cell line (HeLa) obtained from NCCS (National Centre for Cell Science), Pune, India, human colon cancer cell line DLD-1 (ECACC, Salisbury, UK) and

mouse breast cancer cell line 4T1 (ATCC, Manassas, VA) were cultured in RPMI 1640. Human embryonic kidney (HEK-293) cell line was obtained from (ATCC, Manassas, VA) and cultured in EMEM. All media were supplemented with 10% (v/v) fetal bovine serum (FBS) and 1% antibiotic–antimycotic solution. To study the antiproliferative activity of compounds, 10 mM stock solutions of compounds were prepared by dissolving them in DMSO (Sigma St. Louis, MO). MTT assay was done as described by ATCC, Manassas, VA. Briefly, cells were seeded in 96 well plates in 100 μL media per well and incubated overnight. After overnight cell adhesion, various concentrations of compounds dissolved in DMSO were added to cells and DMSO alone was used as vehicle control. Cells were grown for 48h to test the effect of compounds. For MTT assay 10 μL of MTT (5mg/ml) was added to each well and incubated for 3 h. The formazan crystals formed by live cells were dissolved by adding DMSO and shaking until completely dissolved at room temperature. Absorbance was measured at 590 nm on the plate reader (Epoch Microplate Reader, Biotek, USA). The measurement of control cells was defined as 100% growth and the percentage growth inhibition of treated cells was calculated from other measurements. Each experiment was done in triplicate. Percentage inhibition of cell growth (anti proliferative activity) was measured by the formula: [(Absorbance of control cells - Absorbance of inhibitor treated cells)/ Absorbance of control cells] X 100 and reported as average of three independent biological replicates.

4.5.3. Electrophoretic mobility shift assay (EMSA)

EMSA was performed to check the interaction of compound **27** with DNA substrate and hLigI as described previously [14]. Three different oligos were used to generate a double stranded, non-ligatable nicked DNA substrate. One was a 5'-FAM labelled 27-mer oligo with a dideoxy modified 3' end (5'-/56-FAM/GTACTATCTCACTGACATACATAGAC/3ddc/-

3'), where FAM labelling and dideoxy modification was used for easy detection of DNA substrate and for creating the non ligatable nick, respectively. The other two oligos were 25-mer (5'-CTGATCTACCAATCGATCGACGTAC-3') and 52-mer (5'-GTACGTCGATCG ATTGGTAGATCAGGGTCTATGTATGTCAGTGAGATAGTAC-3') which were annealed to form a non-ligatable nicked DNA substrate for ligase I. In EMSA, the reaction volume of 20µL contained 10 pmole of hligI with different concentrations of compound (31.25, 62.5, 125, 250, 500 µM) and 2 pmole non-ligatable nicked DNA substrate in a ligation buffer containing Tris-Cl (50 mM, pH7.5), $MgCl_2$ (10 mM), BSA (0.25 mg/ml), NaCl (100mM), ATP (500 mM) were incubated for two hours on ice. 10µL of native gel buffer (50mM TrisCl pH7.5, 20% glycerol, 0.05% bromophenol blue) was added and samples were separated by electrophoresis in 6.5% native polyacrylamide gel and bands were detected by GE Image Quant LAS4010. Represented graphically after three independent experiments in figure 8.

4.5.4. DNase I protection assay

We performed the DNase I protection assay to test the interaction of compound **27** with DNA as described by Cardew *et al* [51]. For this experiment 100 ng of linearized plasmid DNA (pUC18) was incubated with the DNA intercalating agent doxorubicin at 100 µM concentration and then competed with DAPI, methyl green, ampicillin (all at 500 µM concentration) and compound **27** at three different concentrations (250, 500, 700µM) for 30 min at 37˚C in an incubation buffer similar to ligation buffer. After incubation, 0.0025U of DNase1 was added to the reaction mixture for DNA cleavage and incubated for 5 min at 37˚C. After 5 min, the stop buffer containing 7 M Urea, 20 mM Tris-Cl (pH. 7.5), 50 mM EDTA, 20% glycerol and bromophenol blue, was added to stop the reaction. The samples were then resolved in 1% agarose gel and visualized under UV transilluminator and image captured with GE Image Quant LAS4010.

4.5.5. In vitro cell migration assay

The migration of DLD-1 cells was assessed by the wound healing assay as described by Mishra *et al* [52]. Cells were seeded in 6 well plates and grown at 70-80 % confluence. The wound was created with a 200 μL pipette tip in the middle of the well and then cells were treated with different concentrations of compound **27** for 12, 24 and 36 h. Wound closure was measured after different time intervals and imaged with phase contrast microscopy under an inverted microscope (Ziess Primovert using a 10 x phase contrast objective) and quantified by Image-J software. Average values were represented in graphical form after three independent experiments.

4.5.6. Colony formation assay

Colony formation assay was performed as described previously by Chen *et al* with some modifications [45], 400 cells of DLD-1 cell line were seeded per well in 12 well plates and grown overnight in RPMI media containing 10% FBS. Thereafter, different concentrations (1.25, 2.5 and 5μM) of compound **27** were added and cells were grown for 24 h and 48 h. After the desired time point, the culture medium was replaced with fresh medium and cells were grown for another 10 days, exchanging the medium every third day. To observe the colonies formed, the cells were washed with 1X PBS and stained and fixed with 0.5% crystal violet and 6% glutaraldehyde for 30 min at room temperature. Finally, the excess stain was washed with tap water, plates were dried and images were captured.

4.5.7. Measurement of Apoptosis by Annexin V-FITC assay

To measure compound **27** induced apoptosis in colon cancer DLD-1 cells, we performed Annexin V-FITC staining by using a commercially available kit (BD Biosciences, San Diego, CA). Different concentrations of compound **27** (2.5, 5 and 10μM) were added to DLD-1 cells

for 48 h. After 48 h of treatment, the cells were harvested, washed with cold PBS and stained with Annexin V-FITC and propidium iodide (PI) in binding buffer at room temperature in the dark, according to manufacturer's instructions. Analysis of the stained cells was done by fluorescence-activated cell sorter using a FACS-Calibur instrument (BD Biosciences, San Diego, CA) equipped with CellQuest 3.3 Software and average values were plotted graphically from three independent experiments.

4.5.8. Generation of DLD-1 cell spheroids and study of antiproliferative activity of compound ***27***

DLD-1 spheroids were generated via the 'hanging drop' technique as described previously with some modifications [48, 53]. In short, 5 X 10^3 DLD-1 cells/ 10 μL RPMI was placed on the lid of a non-adhesive PBS containing petri dish. Spheroids were incubated for 3 days at 37˚C, in a 5% CO2 incubator. The spheroids were transferred to 0.7% agarose coated 24 well plates containing 10 % RPMI medium. The medium was exchanged after every third day. After 7 days the spheroids were treated with compound **27** at different concentrations (25, 12.5 and 6.25) for 72 h. Spheroids were stained with staining solution containing 2μg/ml FDA (Fluorescein diacetate) and 20μg/ml PI (Propidium iodide) in PBS and incubated for 20 min in the dark, as previously described [54]. The stained spheroids were washed with PBS and then visualized and imaged under Nikon Eclipse Ti fluorescence microscope.

4.5.9. Molecular modelling studies

To model the binding of compound **27** with hLigI, we performed the *in silico* docking of compound **27** with the crystal structure of hLigI retrieved from the PDB database (PDB ID:1X9N) [15]. The co-crystallized nicked DNA and Adenosine Monophosphate moieties were removed before performing the docking experiments. Subsequently, the hydrogen atoms were added to the protein structure. Finally, the energy minimization was accomplished

applying the Sybyl7.1 software suite [55]. The details of the structure preparation and validation of docking protocol are published by us earlier [26]. The structure of compound **27** was drawn using sketch module of Sybyl7.1 software suite. Further, this structure was minimized using MMFF4 force field by using Sybyl7.1. Docking was performed using the FlexX module of Sybyl7.1 [56].

4.5.10. Statistical analysis

All experiments were performed in triplicate and reported as mean ± SEM. Statistical analysis were performed through the Graph Pad Prism software version 5 (San Diego California USA). For the measurement of DNA ligation, cytotoxicty, EMSA and apoptosis, one-way ANOVA followed by Bonferroni post-test were used to assess the statistical significance between control and treated groups. A value of $p<0.05$ was considered statistically significant. ANOVA showed a significant difference from the control: *($P<0.05$), **($P < 0.01$), ***($P < 0.001$), ns (not significant).

Acknowledgment

The authors acknowledge CSIR-CDRI, Govt. of India, for financial and infrastructural support. Instrumentation facilities from SAIF, CDRI, are gratefully acknowledged. Financial support is also acknowledged from Department of Biotechnology (DBT), Govt. of India (Grant-BT/PR6421/GBD/27/436/2012), the Department of Science and Technology (DST), Govt. of India (Grant-SB/FT/LS-163/2012) and CSIR Network projects GENESIS (BSC0121) and Biopros (BSC0106). We acknowledge Dr. S. P. Singh (Technical Officer), CSIR-CDRI, for technical assistance. The authors are also thankful to Sophisticated Analytical Instrument Facility (SAIF) CDRI, Lucknow, India, for providing spectral analysis data of chemical compounds and for support with cell based flow cytometry experiments. SG is thankful to CSIR, New Delhi for financial support. PM is thankful to DBT for financial

support. AU and PK are thankful to UGC, New Delhi for financial support. This manuscript bears the CDRI manuscript number 116/2017/KVS.

Additional Information-The authors declare no competing financial interests.

ACCEPTED MANUSCRIPT

Captions to illustrations

Figure 1: Strategy for designing indole-chalcone based benzopyran molecules.

Figure 2: Effect of 13 indole-chalcone based benzopyrans on the nick sealing activity of human DNA ligase I. Denaturing gel images showing inhibition of hLigI nick sealing activity in the presence of test compounds at 10 μM concentration and the graphical representation of percentage inhibition of nick sealing activity present in purified hLigI.

Figure 3: Percentage antiproliferative activity of indole-chalcone based benzopyrans in various cancer cell lines (A) MDA-MB-231, (B) DLD-1, (C) HeLa, (D) HepG2 and (E) 4T1. Doxorubicin was used as a control to compare antiproliferative activity.

Figure 4: IC_{50} values of compound **27** in various cancer (MDA-MB-231, DLD-1, HeLa, HepG2 and 4T1) and normal (HEK-293) cell lines.

Figure 5: Cartoon representation of SAR studies shows the groups important for inhibition of DNA nick sealing activity and anti-proliferative activity.

Figure 6: Inhibition of DNA nick sealing (ligation) activity by compound **27** at 3.125, 6.25, 12.5, 25 and 50 μM concentrations against various human (hLigI, hLigIII and hLigIV/XRCC4) and non-human DNA ligases (T4 DNA ligase).

Figure 7: *In silico* docking of compound **27** at the DNA binding site of hLigI (crystal structure 1X9N) represented as a cartoon. Compound **27** is shown in purple sticks, the interacting residues of hLigI are shown as cyan sticks; black dashed lines represent the hydrogen bonds.

Figure 8: Electrophoretic Mobility Shift Assay (EMSA) for compound **27** with DNA-protein complex shows a concentration dependent inhibition of complex formation, suggesting a competitive mode of inhibition.

Figure 9: DNase I protection assay for DNA incubated with compound **27** and various other controls. The representative agarose gel shows that unlike Doxoburicin, Methyl green and DAPI compound **27** was not able to protect DNA from DNase digestion, suggesting that it does not bind to DNA.

Figure 10: Bright field images of DLD-1 cells after treatment with compound **27** at various concentrations (2.5, 5 and 10 µM) for 24 and 48 h shows changes in cellular morphology, indicating cellular stress.

Figure 11: Images of colony formation assay showed inhibition of colony formation by DLD-1 cells in the presence of compound **27** in a dose and time dependent manner.

Figure 12: Bright field images of inhibition of DLD-1 cell migration in the presence of compound **27**. The graph shows significant decrease in % open area in control versus treated cells after different time points, indicating reduced cellular migration.

Figure 13: Induction of apoptosis in DLD-1 cells after treatment of compound **27** at different concentrations for 48 h. The percentage population of early and late apoptotic cells at different concentrations of the compound is represented graphically.

Figure 14: Evaluation of cell viability in 3D spheroids of DLD-1 cells in the presence of compound **27** at different concentrations (from left to right: phase-contrast image, FDA-signal, PI-signal, composite of FDA and PI signal). (Scale bar: 200 µm).

ACCEPTED MANUSCRIPT

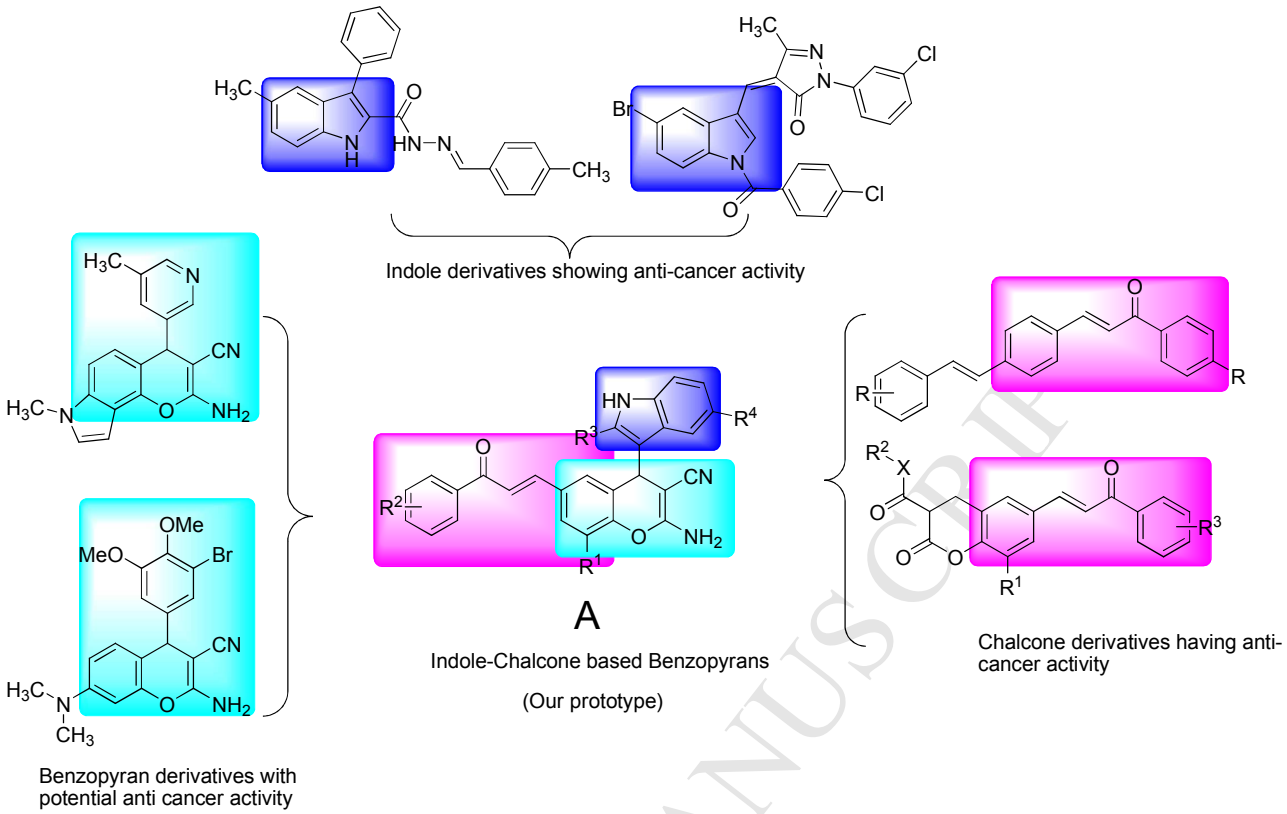

Figure 1: Strategy for designing indole-chalcone based benzopyran hybrids.

ACCEPTED MANUSCRIPT

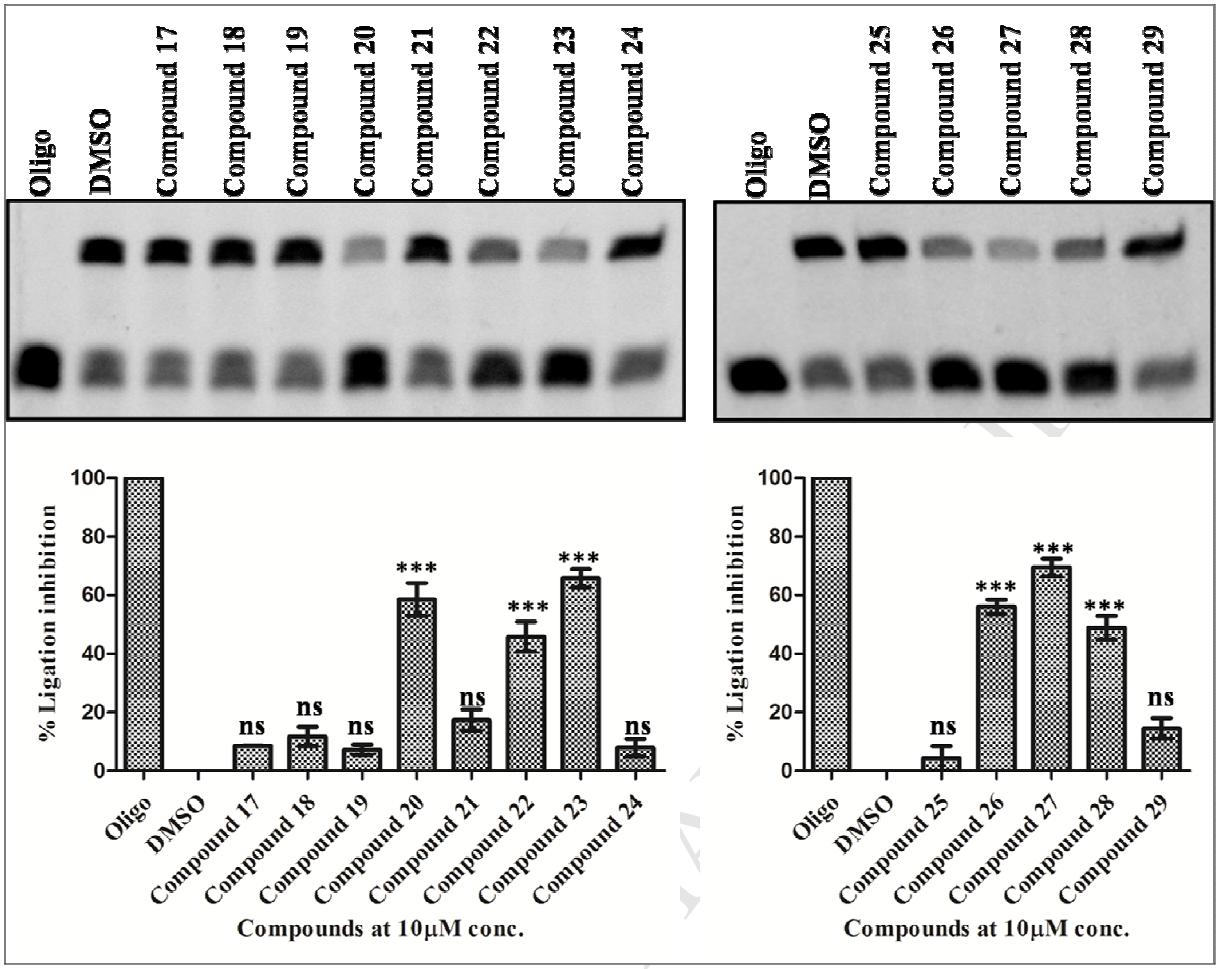

Figure 2: Effect of 13 indole-chalcone based benzopyrans on the nick sealing activity of human DNA ligase I. Denaturing gel images show inhibition of hLigI nick sealing activity in the presence of test compounds at 10 μM concentration and the graphical representation of percentage inhibition of nick sealing activity present in purified hLigI.

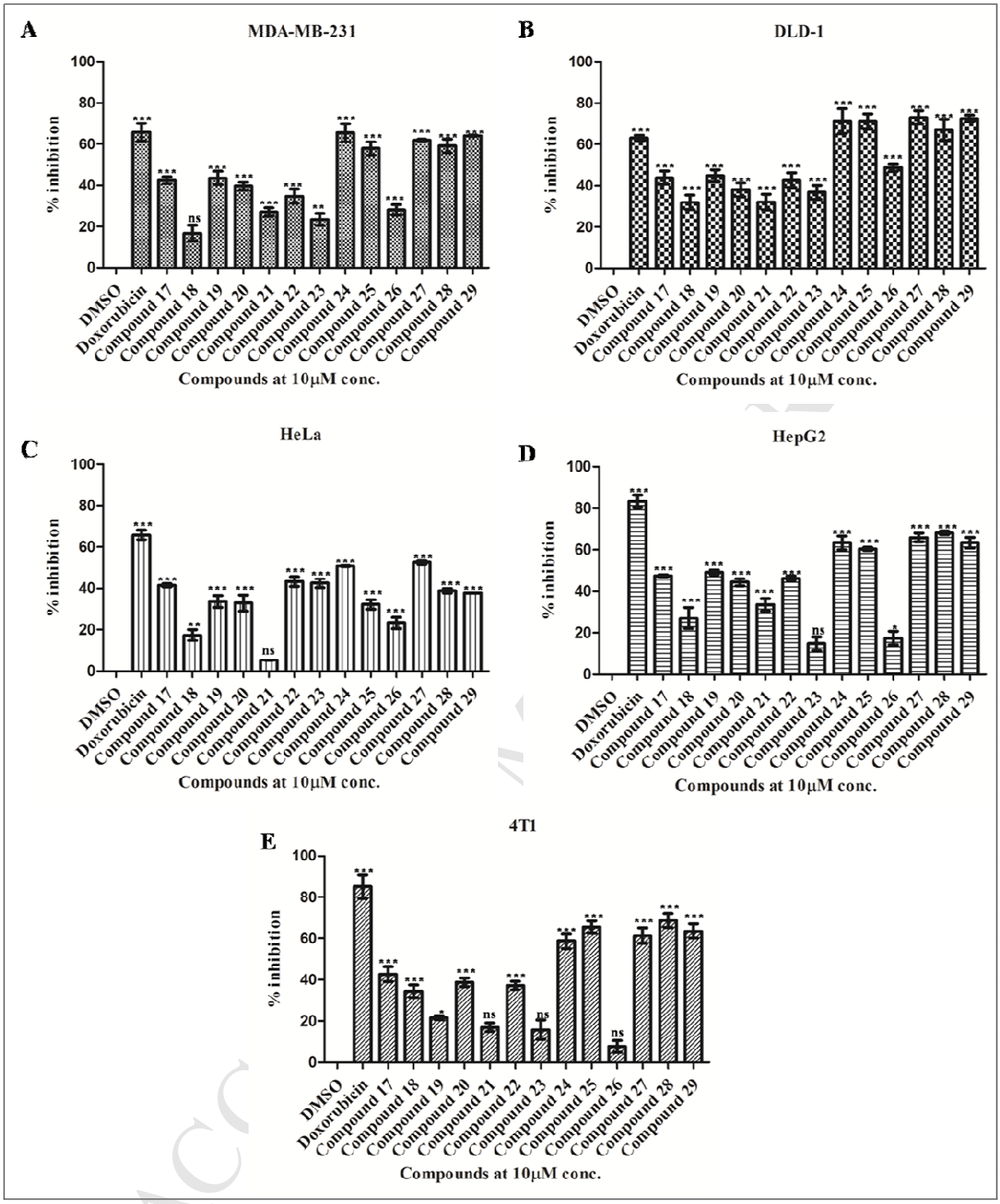

Figure 3: Percentage antiproliferative activity of indole-chalcone based benzopyrans in various cancer cell lines (A) MDA-MB-231, (B) DLD-1, (C) HeLa, (D) HepG2 and (E) 4T1. Doxorubicin was used as a control to compare antiproliferative activity.

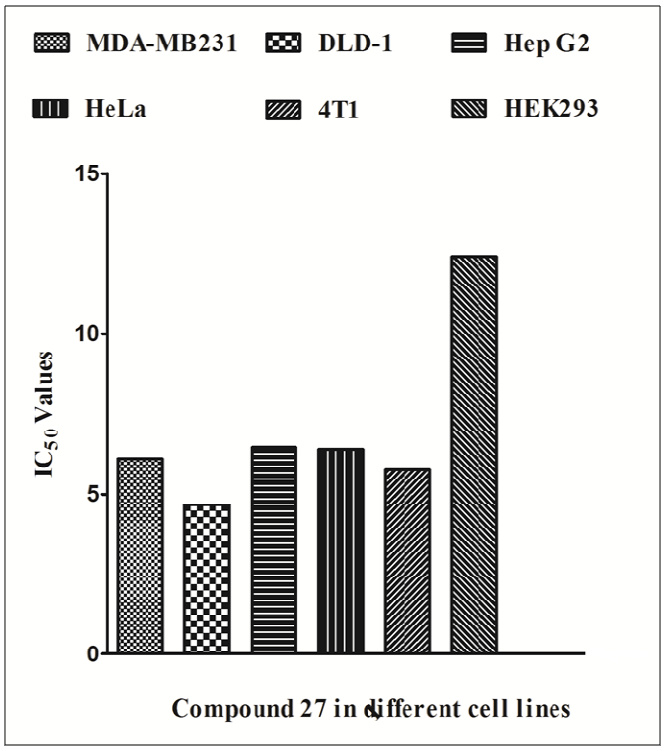

Cell lines	IC_{50} values (µM) of compound 27 in different cell lines
MDA-MB-231	6.090
DLD-1	4.656
HepG2	6.457
HeLa	6.398
4T1	5.756
HEK-293	12.4

Figure 4: IC_{50} values of compound **27** in various cancer (MDA-MB-231, DLD-1, HeLa, HepG2 and 4T1) and normal (HEK-293) cell lines.

ACCEPTED MANUSCRIPT

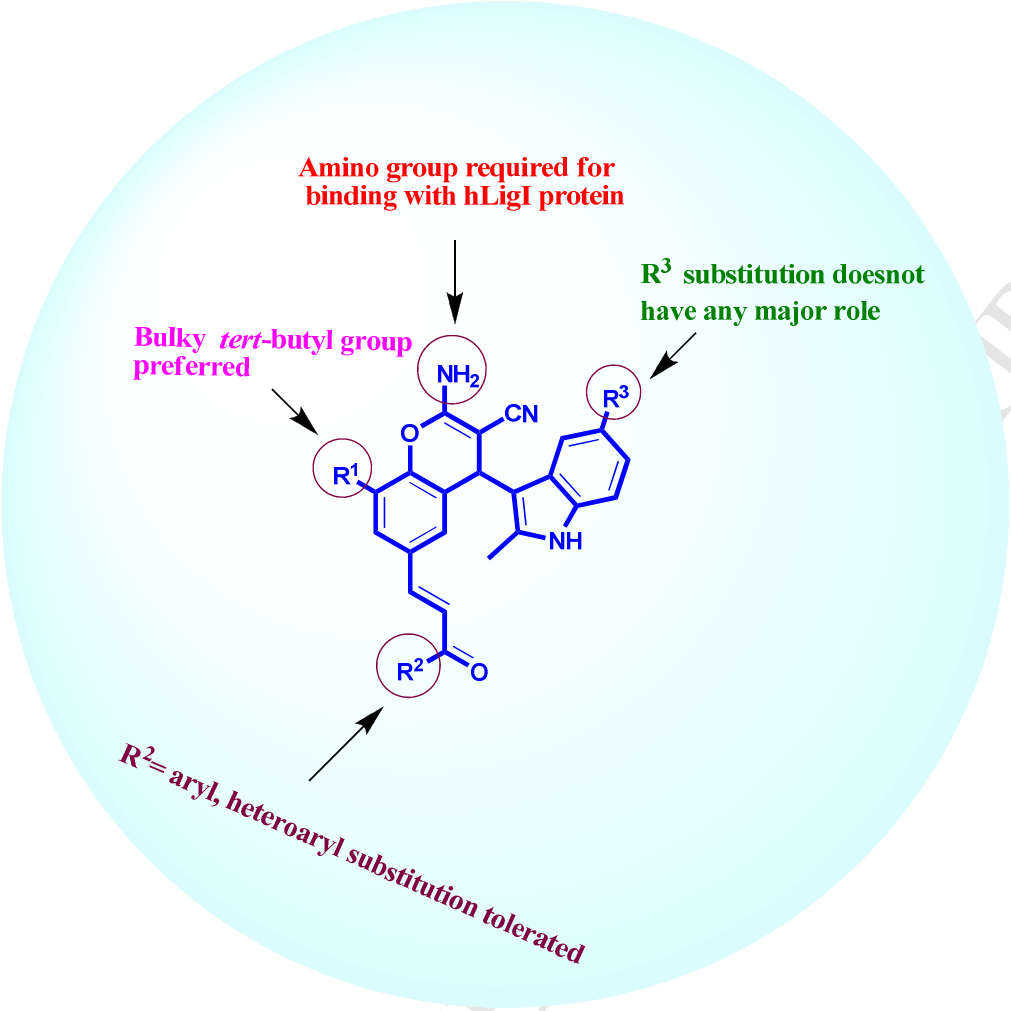

Figure 5: Pictorial representation of SAR studies shows the groups important for inhibition of DNA nick sealing activity and anti-proliferative activity.

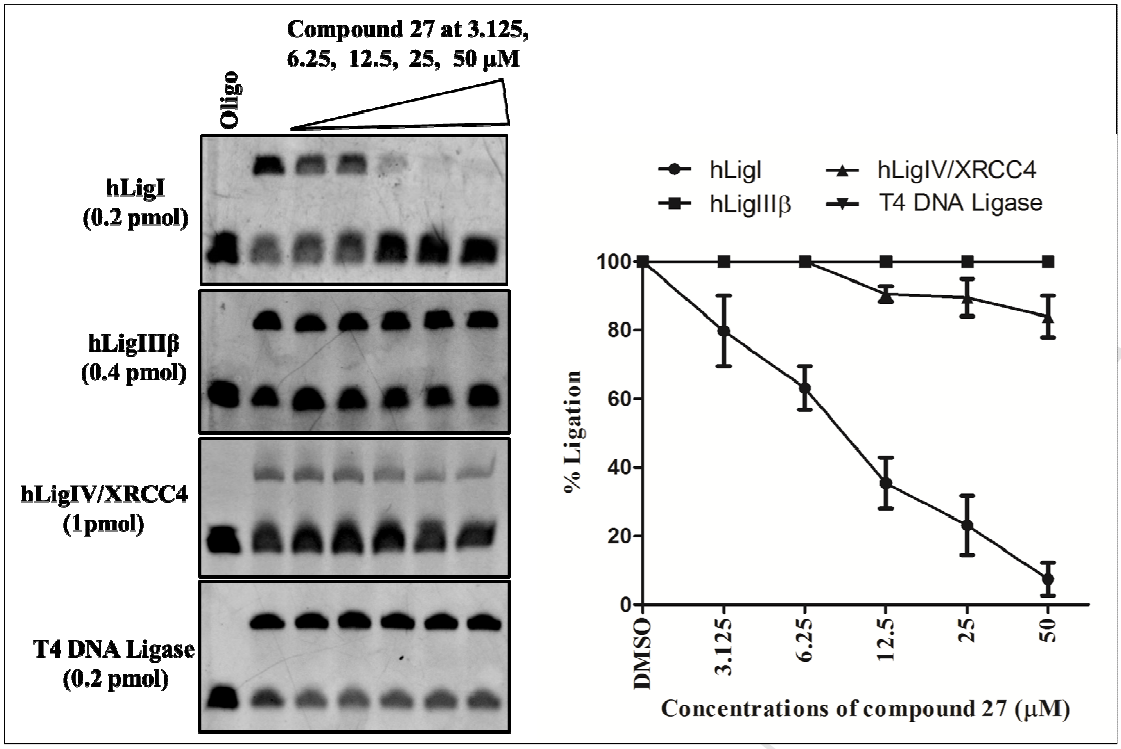

Figure 6: Inhibition of DNA nick sealing (ligation) activity by compound **27** at 3.125, 6.25, 12.5, 25 and 50 µM concentrations against various human (hLigI, hLigIII and hLigIV/XRCC4) and non-human DNA ligases (T4 DNA ligase).

ACCEPTED MANUSCRIPT

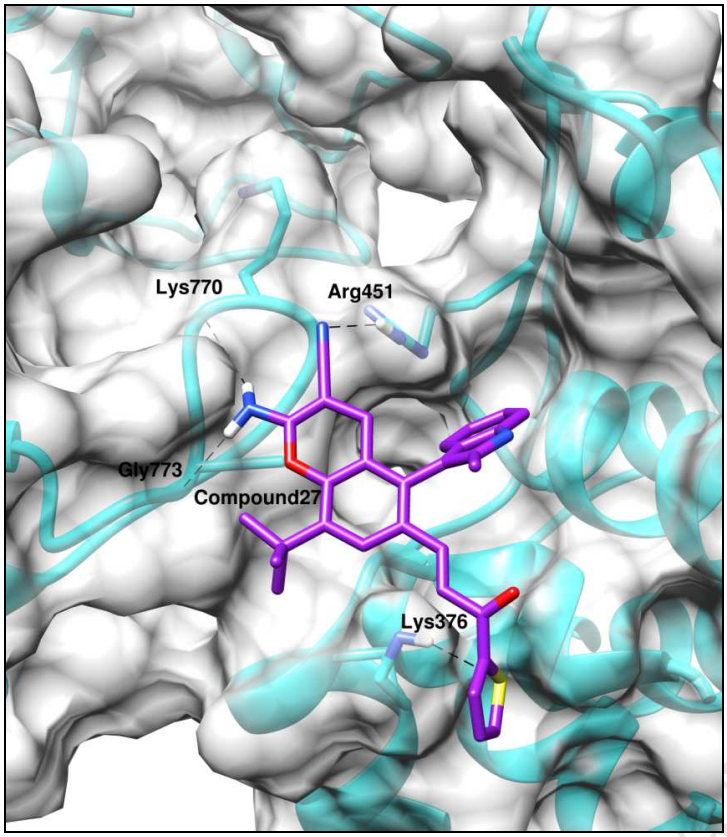

Figure 7: *In silico* docking of compound **27** at the DNA binding site of hLigI (crystal structure 1X9N) represented as a cartoon. Compound **27** is shown in purple sticks, the interacting residues of hLigI are shown as cyan sticks; black dashed lines represent the hydrogen bonds.

ACCEPTED MANUSCRIPT

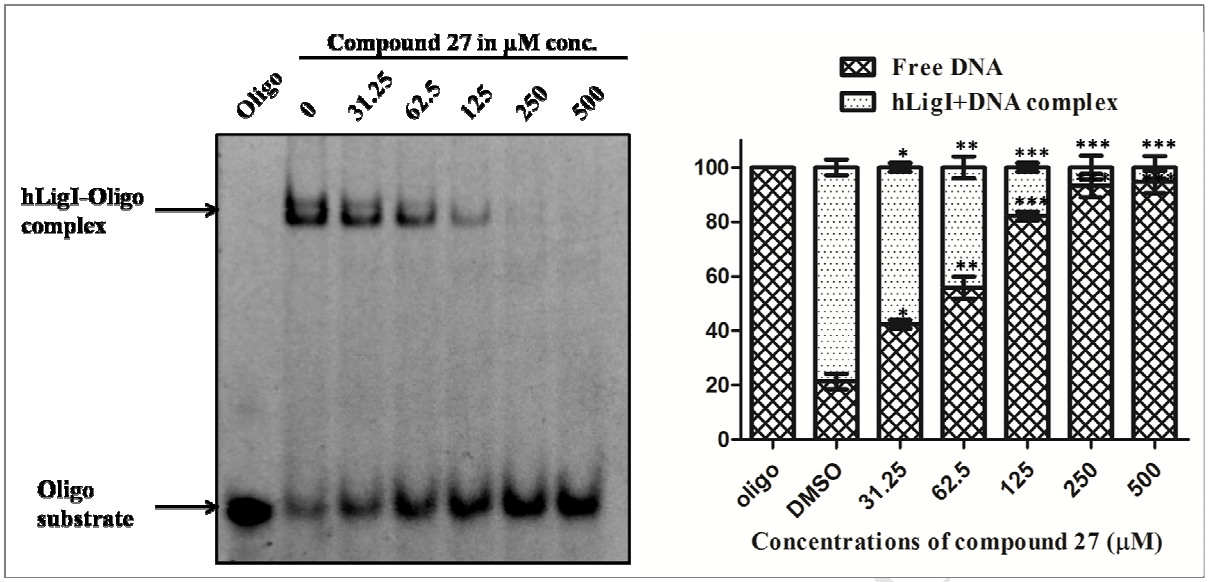

Figure 8: Electrophoretic Mobility Shift Assay (EMSA) for hLig1-DNA complex shows a concentration dependent inhibition of complex formation in the presence of increasing concentrations of compound **27**, suggesting a competitive mode of inhibition.

ACCEPTED MANUSCRIPT

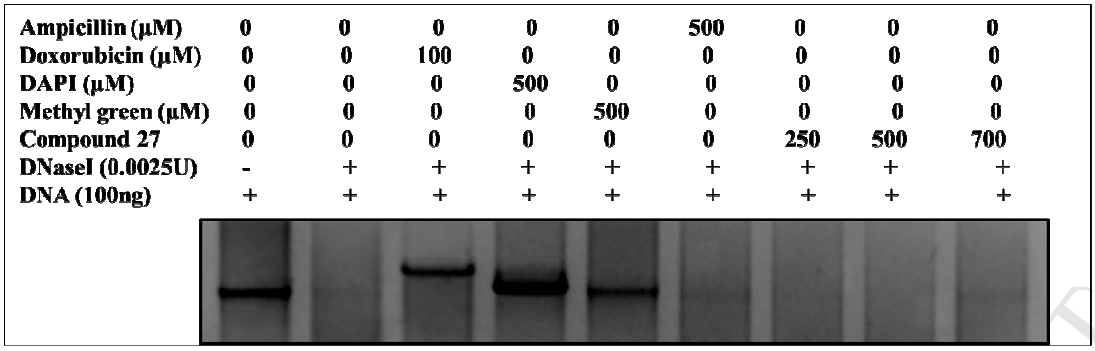

Figure 9: DNase I protection assay for DNA incubated with compound **27** and various other controls. The representative agarose gel shows that unlike Doxoburicin, Methyl green and DAPI compound **27** was not able to protect DNA from DNase digestion, suggesting that it does not bind to DNA.

ACCEPTED MANUSCRIPT

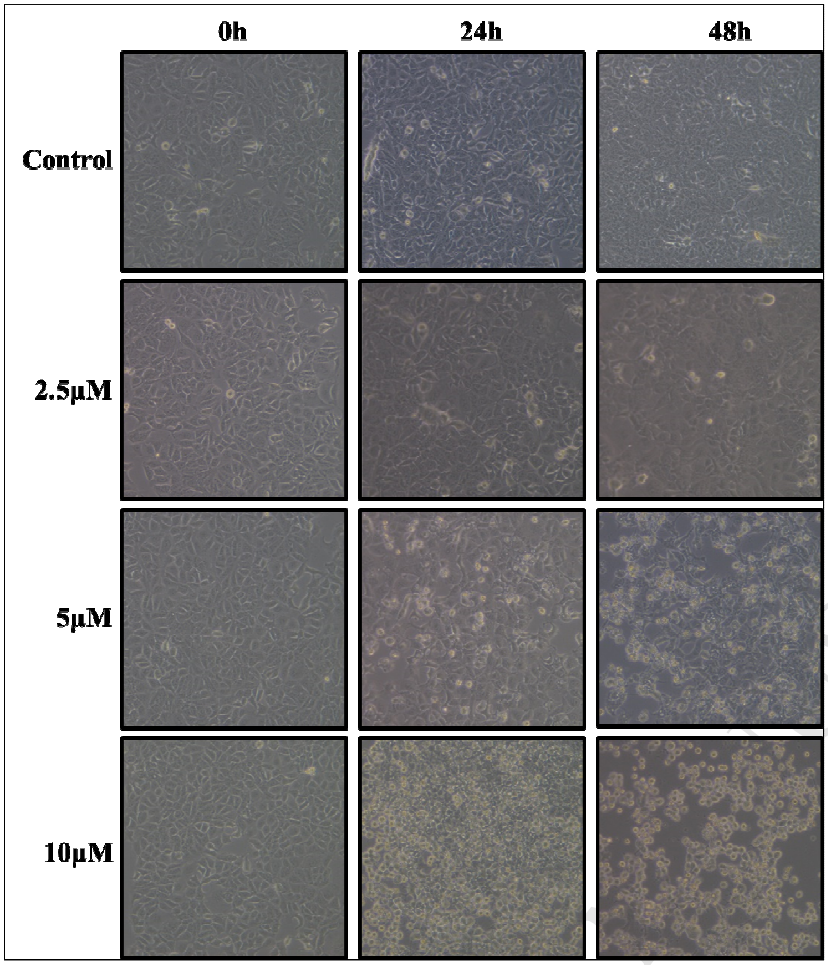

Figure 10: Bright field images of DLD-1 cells after treatment with compound **27** at various concentrations (2.5, 5 and 10 µM) for 24 and 48 h shows changes in cellular morphology, indicating cellular stress.

ACCEPTED MANUSCRIPT

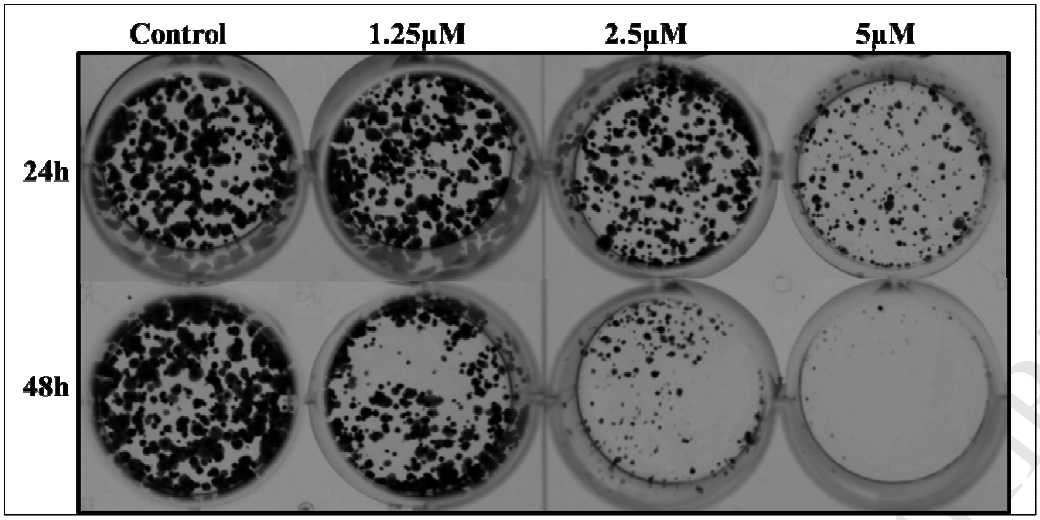

Figure 11: Images of colony formation assay showed inhibition of colony formation by DLD-1 cells in the presence of compound **27** in a dose and time dependent manner.

ACCEPTED MANUSCRIPT

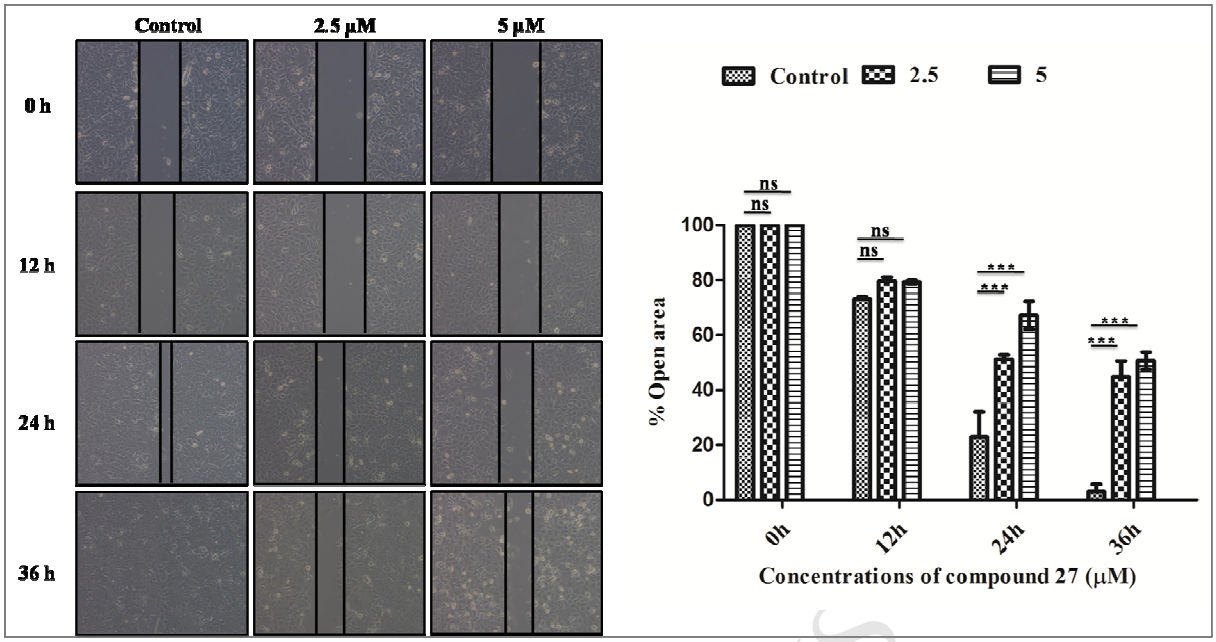

Figure 12: Bright field images show inhibition of migration of DLD-1 cells in the presence of compound **27**. The graph shows significant decrease in % open area in control compared to treated cells after different time points, indicating reduced cellular migration.

ACCEPTED MANUSCRIPT

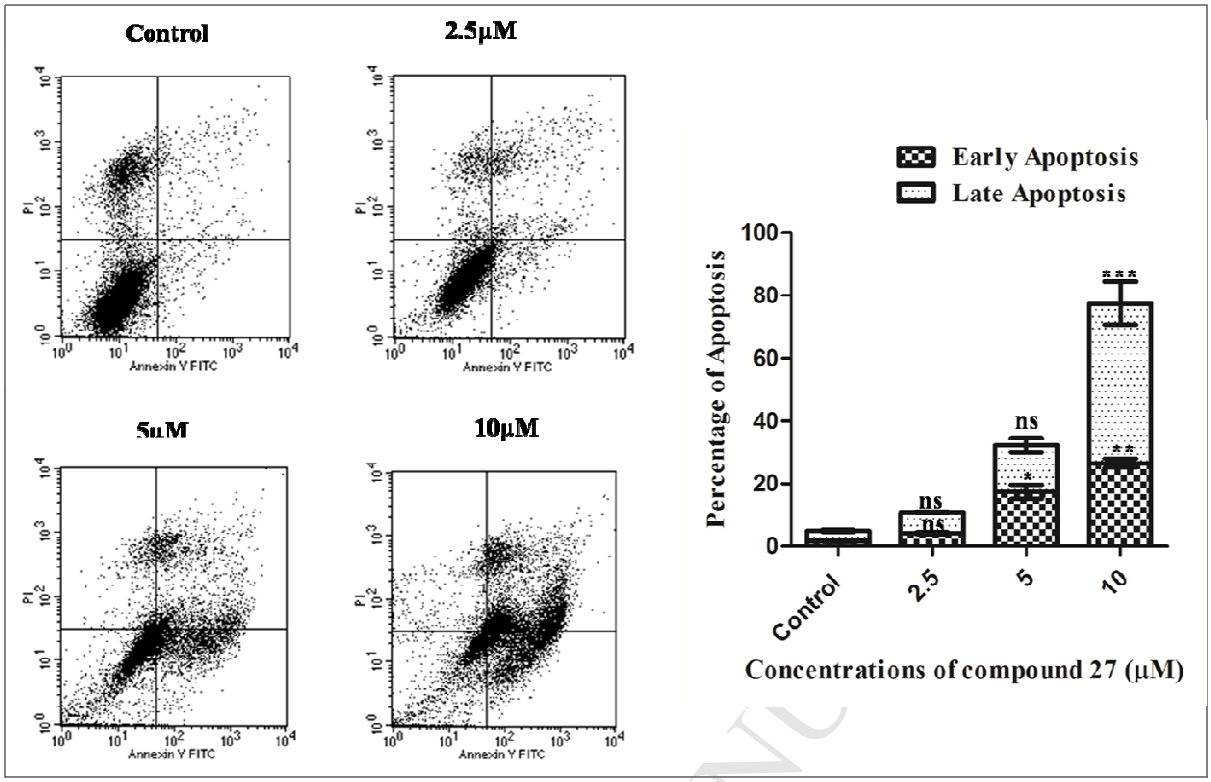

Figure 13: Induction of apoptosis in DLD-1 cells after treatment with compound **27** at different concentrations for 48 h. The percentage population of early and late apoptotic cells at different concentrations of the compound is represented graphically.

ACCEPTED MANUSCRIPT

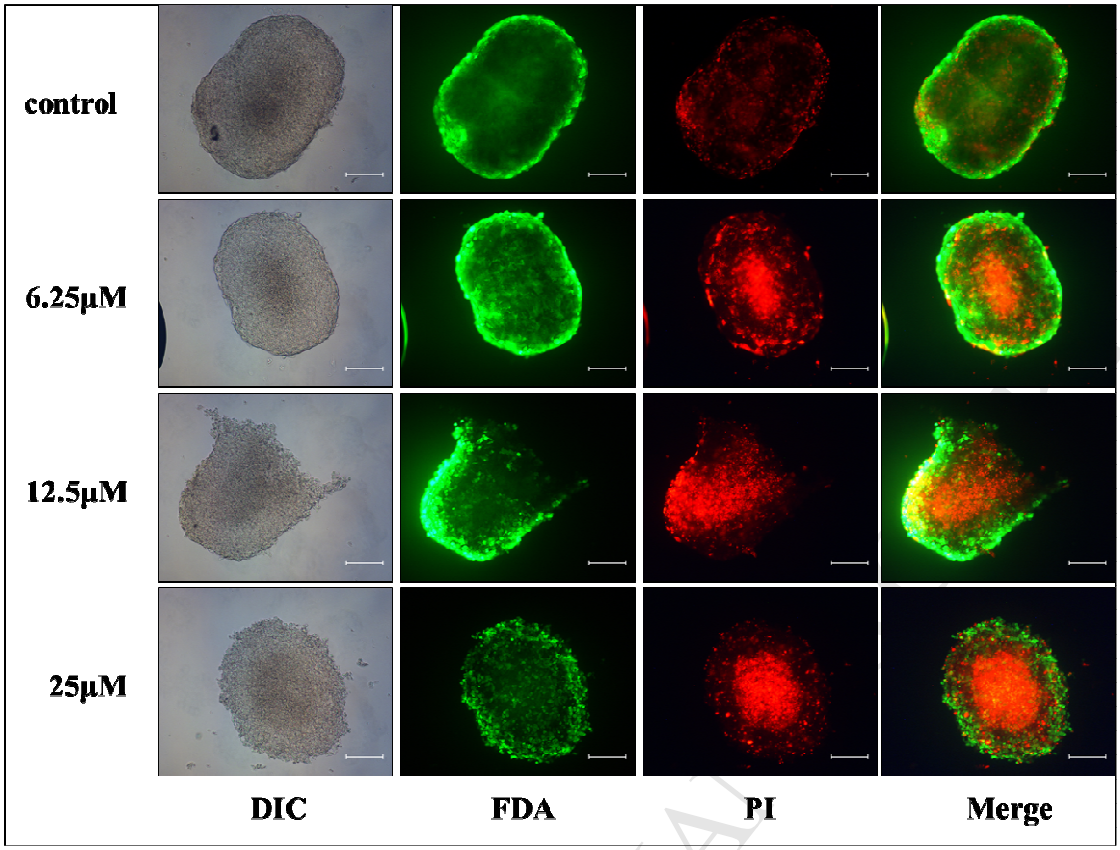

Figure 14: Evaluation of cell viability in 3D spheroids of DLD-1 cells in the presence of compound **27** tested at different concentrations (from left to right: phase-contrast image, FDA-signal, PI-signal, composite of FDA and PI signal). (Scale bar: 200 µm).

ACCEPTED MANUSCRIPT

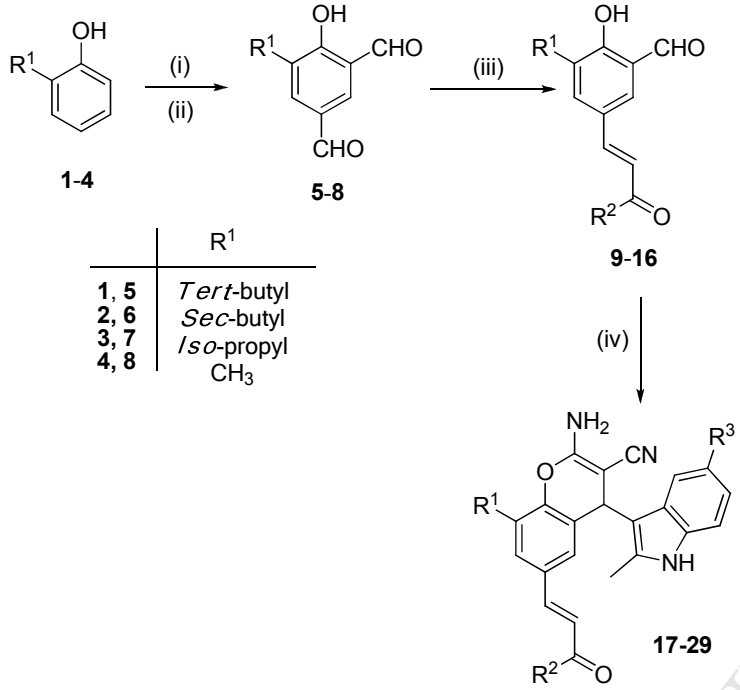

	R^1
1, 5	*Tert*-butyl
2, 6	*Sec*-butyl
3, 7	*Iso*-propyl
4, 8	CH_3

	R^1	R^2
9	*Tert*-butyl	$-C_6H_4(CH_3)$
10	*Tert*-butyl	$-C_6H_4(OMe)$
11	*Tert*-butyl	$-C_6H_2(OMe)_3$
12	*Tert*-butyl	$-C_6H_4(Cl)$
13	*Tert*-butyl	$-C_4H_3S$
14	*Sec*-butyl	$-C_6H_2(OMe)_3$
15	*Iso*-propyl	$-C_4H_3S$
16	CH_3	$-C_4H_3S$

	R^1	R^2	R^3
17	*Tert*-butyl	$-C_6H_4(CH_3)$	—H
18	*Tert*-butyl	$-C_6H_4(OMe)$	—H
19	*Tert*-butyl	$-C_6H_2(OMe)_3$	—H
20	*Tert*-butyl	$-C_6H_4(Cl)$	—H
21	*Sec*-butyl	$-C_6H_2(OMe)_3$	—H
22	*Tert*-butyl	$-C_6H_4(CH_3)$	$-OCH_3$

	R^1	R^2	R^3
23	*Tert*-butyl	$-C_6H_4(CH_3)$	—Cl
24	*Iso*-propyl	$-C_4H_3S$	—H
25	*Iso*-propyl	$-C_4H_3S$	$-OCH_3$
26	*Tert*-butyl	$-C_6H_4(OCH_3)$	—Cl
27	*Tert*-butyl	$-C_4H_3S$	—H
28	CH_3	$-C_4H_3S$	—H
29	*Tert*-butyl	$-C_4H_3S$	$-OCH_3$

Scheme 1: Reagents and Conditions: (i) HMTA, TFA, 120 °C, 4h, (ii) aq H_2SO_4, 100 °C, 2 h, (iii) different acetophenone derivatives, Conc. HCl, dioxane, 8 h, reflux, (iv) malononitrile, indole derivative, acetonitrile 6 h reflux.

ACCEPTED MANUSCRIPT

References

1. S.P. Jackson, J. Bartek, The DNA-damage response in human biology and disease, Nature 461 (2009) 1071-1078.

2. J.J. Blow, R.A. Laskey, A role for the nuclear envelope in controlling DNA replication within the cell cycle, Nature 332 (1988) 546-548.

3. I. Frouin, A. Montecucco, S. Spadari, G. Maga, DNA replication: a complex matter, EMBO reports 4 (2003) 666-670.

4. K.V. Sashidhara, L.R. Singh, M. Shameem, S. Shakya, A. Kumar, T.S. Laxman, S. Krishna, M.I. Siddiqi, R.S. Bhatta, D. Banerjee, Design, synthesis and anticancer activity of dihydropyrimidinone-semicarbazone hybrids as potential human DNA ligase 1 inhibitors, Med. Chem. Commun. 7 (2016) 2349-2363.

5. K.W. Caldecott, Single-strand break repair and genetic disease, Nat. Rev. Genet. 9 (2008) 619-631.

6. R. Okazaki, T. Okazaki, K. Sakabe, K. Sugimoto, A. Sugino, Mechanism of DNA chain growth. I. Possible discontinuity and unusual secondary structure of newly synthesized chains, Proc. Natl. Acad. Sci. U S A 59 (1968) 598-605.

7. I.R. Lehman, DNA ligase: structure, mechanism, and function, Science 186 (1974) 790-797.

8. A.L. Deshmukh, C. Kumar, D.K. Singh, P. Maurya, D. Banerjee, Dynamics of replication proteins during lagging strand synthesis: A crossroads for genomic instability and cancer, DNA repair 42 (2016) 72-81.

9. F. Dietlein, L. Thelen, H.C. Reinhardt, Cancer-specific defects in DNA repair pathways as targets for personalized therapeutic approaches, Trends Genet. 30 (2014) 326-339.

10. D. Leibeling, P. Laspe, S. Emmert, Nucleotide excision repair and cancer, J. Mol. Histol. 37 (2006) 225-238.

11. A. Torgovnick, B. Schumacher, DNA repair mechanisms in cancer development and therapy, Front. Genet. 6 (2015) 157.

12. H. Teraoka, M. Sawai, K. Yamamoto, K. Tsukada, DNA ligase I mRNA and enzyme levels in human hematopoietic cells under dimethyl sulfoxide-induced growth-arrest and differentiation, Biochem. Int. 26 (1992) 963-971.

13. D. Sun, R. Urrabaz, M. Nguyen, J. Marty, S. Stringer, E. Cruz, L. Medina-Gundrum, S. Weitman, Elevated expression of DNA ligase I in human cancers, Clin. Cancer Res. 7 (2001) 4143-4148.

14. D.K. Singh, M.K. Hussain, S. Krishna, A.L. Deshmukh, M. Shameem, P. Maurya, K. Hajela, M.I. Siddiqi, D. Banerjee, Identification of a novel human DNA ligase I inhibitor that promotes cellular apoptosis in DLD-1 cells: an in silico and in vitro mechanistic study, Rsc Adv. 6 (2016) 94574-94587.

15. J.M. Pascal, P.J. O'Brien, A.E. Tomkinson, T. Ellenberger, Human DNA ligase I completely encircles and partially unwinds nicked DNA, Nature 432 (2004) 473-478.

16. J. Moser, H. Kool, I. Giakzidis, K. Caldecott, L.H.F. Mullenders, M.I. Fousteri, Sealing of chromosomal DNA nicks during nucleotide excision repair requires XRCC1 and DNA ligase III alpha in a cell-cycle-specific manner, Mol. Cell 27 (2007) 311-323.

17. A.B. Robertson, A. Klungland, T. Rognes, I. Leiros, DNA Repair in Mammalian Cells, Cell Mol. Life Sci. 66 (2009) 981-993.

18. G.L. Dianov, Base excision repair targets for cancer therapy, Am. J. Cancer Res. 1 (2011) 845-851.

19. L. Liang, L. Deng, S.C. Nguyen, X. Zhao, C.D. Maulion, C.S. Shao, J.A. Tischfield, Human DNA ligases I and III, but not ligase IV, are required for microhomology-mediated end joining of DNA double-strand breaks, Nucleic Acids Res. 36 (2008) 3297-3310.

20. D.K. Singh, S. Krishna, S. Chandra, M. Shameem, A.L. Deshmukh, D. Banerjee, Human DNA Ligases: A Comprehensive New Look for Cancer Therapy, Med. Res. Rev. 34 (2014) 567-595.

21. T.E. Wilson, U. Grawunder, M.R. Lieber, Yeast DNA ligase IV mediates non-homologous DNA end joining, Nature 388 (1997) 495-498.

22. L.M. Henderson, C.F. Arlett, S.A. Harcourt, A.R. Lehmann, B.C. Broughton, Cells from an immunodeficient patient (46BR) with a defect in DNA ligation are hypomutable but hypersensitive to the induction of sister chromatid exchanges, Proc. Natl. Acad. Sci. U S A 82 (1985) 2044-2048.

23. D.E. Barnes, A.E. Tomkinson, A.R. Lehmann, A.D. Webster, T. Lindahl, Mutations in the DNA ligase I gene of an individual with immunodeficiencies and cellular hypersensitivity to DNA-damaging agents, Cell 69 (1992) 495-503.

24. S. Das-Bradoo, H.D. Nguyen, J.L. Wood, R.M. Ricke, J.C. Haworth, A.K. Bielinsky, Defects in DNA ligase I trigger PCNA ubiquitylation at Lys 107, Nat. Cell Biol. 12 (2010) 74-79.

25. A. Montecucco, G. Biamonti, E. Savini, F. Focher, S. Spadari, G. Ciarrocchi, DNA ligase I gene expression during differentiation and cell proliferation, Nucleic Acids Res. 20 (1992) 6209-6214.

26. S. Krishna, D.K. Singh, S. Meena, D. Datta, M.I. Siddiqi, D. Banerjee, Pharmacophore-based screening and identification of novel human ligase I inhibitors with potential anticancer activity, J. Chem. Inf. Model 54 (2014) 781-792.

27. M. Shameem, R. Kumar, S. Krishna, C. Kumar, M.I. Siddiqi, B. Kundu, D. Banerjee, Synthetic modified pyrrolo[1,4] benzodiazepine molecules demonstrate selective anticancer activity by targeting the human ligase 1 enzyme: An in silico and in vitro mechanistic study, Chem. Biol. Interact. 237 (2015) 115-124.

28. E. Vitaku, D.T. Smith, J.T. Njardarson, Analysis of the structural diversity, substitution patterns, and frequency of nitrogen heterocycles among U.S. FDA approved pharmaceuticals, J. Med. Chem. 57 (2014) 10257-10274.

29. H.Z. Zhang, J. Drewe, B. Tseng, S. Kasibhatla, S.X. Cai, Discovery and SAR of indole-2-carboxylic acid benzylidene-hydrazides as a new series of potent apoptosis inducers using a cell-based HTS assay, Bioorg. Med. Chem. 12 (2004) 3649-3655.

30. Shaveta, P. Singh, Structural optimization of indole based compounds for highly promising anti-cancer activities: structure activity relationship studies and identification of lead molecules, Eur. J. Med. Chem. 74 (2014) 440-450.

31. R. Kant, D. Kumar, D. Agarwal, R.D. Gupta, R. Tilak, S.K. Awasthi, A. Agarwal, Synthesis of newer 1,2,3-triazole linked chalcone and flavone hybrid compounds and evaluation of their antimicrobial and cytotoxic activities, Eur. J. Med. Chem. 113 (2016) 34-49.

32. A. Hammuda, R. Shalaby, S. Rovida, D.E. Edmondson, C. Binda, A. Khalil, Design and synthesis of novel chalcones as potent selective monoamine oxidase-B inhibitors, Eur. J. Med. Chem. 114 (2016) 162-169.

33. S. Kraege, K. Stefan, K. Juvale, T. Ross, T. Willmes, M. Wiese, The combination of quinazoline and chalcone moieties leads to novel potent heterodimeric modulators of breast cancer resistance protein (BCRP/ABCG2), Eur. J. Med. Chem. 117 (2016) 212-229.

34. S.P. Bahekar, S.V. Hande, N.R. Agrawal, H.S. Chandak, P.S. Bhoj, K. Goswami, M.V. Reddy, Sulfonamide chalcones: Synthesis and in vitro exploration for therapeutic potential against Brugia malayi, Eur. J. Med. Chem. 124 (2016) 262-269.

35. D. Kumar, K.K. Raj, S.V. Malhotra, D.S. Rawat, Synthesis and anticancer activity evaluation of resveratrol-chalcone conjugates, Med. Chem. Commun. 5 (2014) 528-535.

36. K.V. Sashidhara, A. Kumar, M. Kumar, J. Sarkar, S. Sinha, Synthesis and in vitro evaluation of novel coumarin-chalcone hybrids as potential anticancer agents, Bioorg. Med. Chem. Lett. 20 (2010) 7205-7211.

37. S.X. Cai, S. Jiang, W. Kemnitzer, H. Zhang, G. Attardo, R. Denis, Substituted 4-aryl-4H-chromenes and analogs as activators of caspases and inducers of apoptosis and the use thereof, PCT Int. Appl. 2003, WO 2003097806 A2 20031127.

38. W. Kemnitzer, J. Drewe, S. Jiang, H. Zhang, C. Crogan-Grundy, D. Labreque, M. Bubenick, G. Attardo, R. Denis, S. Lamothe, H. Gourdeau, B. Tseng, S. Kasibhatla, S.X. Cai, Discovery of 4-aryl-4H-chromenes as a new series of apoptosis inducers using a cell- and caspase-based high throughput screening assay. 4. Structure-activity relationships of N-alkyl substituted pyrrole fused at the 7,8-positions, J. Med. Chem. 51 (2008) 417-423.

39. K.V. Sashidhara, R.K. Modukuri, S. Singh, K. Bhaskara Rao, G. Aruna Teja, S. Gupta, S. Shukla, Design and synthesis of new series of coumarin-aminopyran derivatives possessing potential anti-depressant-like activity, Bioorg. Med. Chem. Lett. 25 (2015) 337-341.

40. K.V. Sashidhara, L.R. Singh, D. Choudhary, A. Arun, S. Gupta, S. Adhikary, G.R. Palnati, R. Konwar, R. Trivedi, Design, synthesis and in vitro evaluation of coumarin-imidazo[1,2-a]pyridine derivatives against cancer induced osteoporosis, RSC Adv. 6 (2016) 80037-80048.

41. W. Kemnitzer, J. Drewe, S. Jiang, H. Zhang, C. Crogan-Grundy, D. Labreque, M. Bubenick, G. Attardo, R. Denis, S. Lamothe, H. Gourdeau, B. Tseng, S. Kasibhatla, S.X. Cai, Discovery of 4-aryl-4H-chromenes as a new series of apoptosis inducers using a cell- and caspase-based high throughput screening assay. 4. Structure-activity relationships of N-alkyl substituted pyrrole fused at the 7,8-positions, J. Med. Chem. 51 (2008) 417-423.

42. D. Jiang, X.J. Pan, M.H. Li, Y.L. Gu, 2-Methylindole as an Indicative Nucleophile for Developing a Three-Component Reaction of Aldehyde with Two Different Nucleophiles, Acs Comb Sci. 16 (2014) 287-292.

43. N.C. Ganguly, S. Roy, P. Mondal, R. Saha, An efficient one-pot organocatalytic synthesis of 9-(1H-indol-3-yl)-xanthen-4-(9H)-ones under mild aqueous micellar conditions, Tetrahedron Lett. 53 (2012) 7067-7071.

44. S. Zhong, X. Chen, X. Zhu, B. Dziegielewska, K.E. Bachman, T. Ellenberger, J.D. Ballin, G.M. Wilson, A.E. Tomkinson, A.D. MacKerell, Jr., Identification and validation of human DNA ligase inhibitors using computer-aided drug design, J. Med. Chem. 51 (2008) 4553-4562.

45. X. Chen, S.J. Zhong, Y. Zhu, B. Dziegielewska, T. Ellenberger, G.M. Wilson, A.D. MacKerell, A.E. Tomkinson, Rational design of human DNA ligase inhibitors that target cellular DNA replication and repair, Cancer. Res. 68 (2008) 3169-3177.

46. L.G. Rodriguez, X. Wu, J.L. Guan, Wound-healing assay, Methods Mol. Biol. 294 (2005) 23-29.

47. J. Friedrich, C. Seidel, R. Ebner, L.A. Kunz-Schughart, Spheroid-based drug screen: considerations and practical approach, Nat. Protoc. 4 (2009) 309-324.

48. M. Zanoni, F. Piccinini, C. Arienti, A. Zamagni, S. Santi, R. Polico, A. Bevilacqua, A. Tesei, 3D tumor spheroid models for in vitro therapeutic screening: a systematic approach to enhance the biological relevance of data obtained, Sci. Rep. 6 (2016).

49. K.V. Sashidhara, K.B. Rao, V. Kushwaha, R.K. Modukuri, R. Verma, P.K. Murthy, Synthesis and antifilarial activity of chalcone-thiazole derivatives against a human lymphatic filarial parasite, Brugiamalayi, Eur. J. Med. Chem. 81 (2014) 473-480.

50. A. Ganesan, J. Kothandapani, S.G. Subramaniapillai, Extending the scope of oleic acid catalysis in diversity-oriented synthesis of chromene and pyrimidine based scaffolds, Rsc Adv. 6 (2016) 20582-20587.

51. S. Cardew and K. R. Fox, DNase I footprinting Methods, Mol. Biol. (2010) 613, 153–172.

52. T. Mishra, R.K. Arya, S. Meena, P. Joshi, M. Pal, B. Meena, D.K. Upreti, T.S. Rana, D. Datta, Isolation, Characterization and Anticancer Potential of Cytotoxic Triterpenes from Betula utilis Bark, PloS one 11 (2016) e0159430.

53. H. Vorsmann, F. Groeber, H. Walles, S. Busch, S. Beissert, H. Walczak, D. Kulms, Development of a human three-dimensional organotypic skin-melanoma spheroid model for in vitro drug testing, Cell Death Dis 4 (2013) e719.

54. K.F. Chambers, E.M.O. Mosaad, P.J. Russell, J.A. Clements, M.R. Doran, 3D Cultures of Prostate Cancer Cells Cultured in a Novel High-Throughput Culture Platform Are More Resistant to Chemotherapeutics Compared to Cells Cultured in Monolayer, Plos One 9 (2014) e111029.

55. M. Rarey, B. Kramer, T. Lengauer, G. Klebe, A fast flexible docking method using an incremental construction algorithm, J. Mol. Biol. 261 (1996) 470-489.

56. Sybyl, version 7.1; Tripos, Inc.: St. Louis, MO, 2005.

ACCEPTED MANUSCRIPT

ACCEPTED MANUSCRIPT

Research Highlights

- Indole-chalcone based benzopyrans were synthesised via multicomponent reaction.
- Compound 27 possessed both antiligase and antiproliferative activity.
- It induces apoptosis and is effective against 3D spheroid culture of DLD-1 cells.

ACCEPTED MANUSCRIPT